Relativistic (Dirac equation) effects in microscopic elastic scattering calculations

M. V. Hynes
Los Alamos National Laboratory, Los Alamos, New Mexico 87545

A. Picklesimer
Department of Physics, University of Maryland, College Park, Maryland 20742
and Los Alamos National Laboratory, Los Alamos, New Mexico 87545

P. C. Tandy
Department of Physics, Kent State University, Kent, Ohio 44242
and Los Alamos National Laboratory, Los Alamos, New Mexico 87545

R. M. Thaler
Department of Physics, Case Western Reserve University, Cleveland, Ohio 44106
and Los Alamos National Laboratory, Los Alamos, New Mexico 87545

(Received 16 October 1984)

A simple relativistic extension of the first-order multiple scattering mechanism for the optical potential is employed within the context of a Dirac equation description of elastic nucleon-nucleus scattering. A formulation of this problem in terms of a momentum-space integral equation displaying an identifiable nonrelativistic sector is described and applied. Extensive calculations are presented for proton scattering from ^{40}Ca and ^{16}O at energies between 100 and 500 MeV. Effects arising from the relativistic description of the propagation of the projectile are isolated and are shown to be responsible for most of the departures from typical nonrelativistic (Schrödinger) results. Off-shell and nonlocal effects are included and these, together with uncertainties in the nuclear densities, are shown not to compromise the characteristic improvement of forward angle spin observable predictions provided by the relativistic approach. The sensitivity to ambiguities in the Lorentz scalar and vector composition of the optical potential is displayed and discussed.

I. INTRODUCTION

In an earlier work,[1] several microscopic aspects of the nonrelativistic impulse approximation (NRIA) to the optical potential for elastic proton scattering from nuclei were studied. In particular, the influence of off-shell and nonlocal effects and the related ambiguities associated with approximate treatments of the nuclear matrix element of two-body scattering operators were investigated. The effect of uncertainties due to incomplete knowledge of nuclear densities was also studied. The scattering observables at forward angles are not affected significantly by these sources of ambiguities in current approximation methods for implementing the NRIA.

Although the NRIA yields qualitatively adequate theoretical predictions, especially at several hundred MeV, these predictions do not provide completely satisfactory descriptions of the high precision data currently available. In particular, some details of the spin observables are poorly given by the NRIA and even the descriptions of differential cross sections are not completely satisfactory when measured against the standards set by the data. Moreover, the successes and failures of the NRIA do not generally appear to follow any systematic dependence upon projectile energy or momentum transfer which might be attributed to higher-order effects, although the difficulties for differential cross sections do diminish as the projectile energy increases. Thus, one cannot readily appeal to what have become the standard sources of error for an "explanation" of the inadequacy of the NRIA. It appears that there may be an omission of a fundamentally important process in the theoretical approach itself. Recent calculations[2] strongly suggest that an approach within the context of a Dirac wave equation may go a long way towards a resolution of this problem. In this paper we address a relativistic approach of this type and present calculations based on a formulation which keeps the relation with the nonrelativistic description in focus.

The unsatisfactory predictions of the NRIA for certain of the low momentum transfer spin observables are especially suggestive, since higher-order correlation effects in the multiple scattering series are expected to be very small for low momentum transfer. Thus, the nature of the difficulties appears to require an additional optical potential contribution which involves all of the target nucleons coherently, such as is obtained in the ground state matrix element of the sum of two-nucleon transition operators. As is described in the following, this sort of additional effect arises rather naturally when the scattering dynamics is described by a Dirac rather than a Schrödinger equation. The enlargement of the Hilbert space to include negative energy intermediate states of the projectile, which is implicit in the use of a Dirac rather than a Schrödinger equation, provides this additional coherent contribution to the optical potential.[3,4]

In order to appreciate the basis of the preceding remarks, it is only necessary to recognize that the idea of coherence[5] underlies the rationale for the development of

a multiple scattering expansion of the optical potential. This can be illustrated by consideration of the first-order ($t\rho$) or impulse approximation term for the optical potential within the simple model of a Slater determinant description of the target states. Consider first the difference between the matrix elements $\langle\phi \mid t_{01} \mid \phi\rangle$ and $\langle\phi_* \mid t_{01} \mid \phi\rangle$, where t_{01} represents the interaction between the projectile (0) and one of the A target nucleons (1), $\mid \phi\rangle$ is the ground state Slater determinant normalized to unity, and $\langle\phi_* \mid$ is, for example, a one-particle—one-hole excited state Slater determinant. With differences in the spatial distributions of each state ignored, the second (inelastic) matrix element is smaller than the first (elastic) matrix element by a statistical factor of $1/A$. This is because in the first matrix element the single particle orbital of particle (1) cannot change and all A of the orbitals contribute, while in the second matrix element orthogonality permits a contribution only from the single term in which particle (1) is in the excited orbital of the final Slater determinant.

The result of employing a given approximate optical potential in a Lippman-Schwinger—type of integral equation for the transition amplitude can be considered from the point of view of a summation of the scattering processes in which the target remains in its ground state. With a first-order optical potential, the second term in the expansion of the Lippmann-Schwinger equation for the transition amplitude is bilinear in the elastic matrix elements already discussed. The size of this term is the appropriate reference scale against which the size of the omitted second-order term for the optical potential should be judged. This omitted term involves scattering through an intermediate excited state and is bilinear in the inelastic matrix elements already discussed. For a given one-particle—one-hole excited state, the ratio of the bilinear term retained for the transition amplitude to that omitted is[6] then $1/A^2$, or $1/A^4$ in the cross section. These simple considerations reinforce the physical usefulness of organizing a theory of the optical potential in orders of multiple scattering. Even for nuclei as light as ^{16}O, this suppression is a large effect. Although there are many excited states that will be coupled to the elastic channel, only a limited sampling will be important at small momentum transfer where the statistical suppression already estimated should be reasonable. At high momentum transfer where the elastic nuclear form factor has fallen many decades, the inelastic terms may be non-negligible, but for low momentum transfer the first-order optical potential should be totally dominant due to the foregoing coherence argument. The consideration of a complete inelastic spectrum orthogonal to the ground state single particle orbitals will introduce the pair correlation function as the centerpiece of this discussion. The suppressions inherent in this quantity for very small momentum transfers are a reflection of the statistical suppression factor already mentioned. Significant departures from the scattering results of the first-order approximation to the optical potential at low momentum transfer would have to come from additional processes that are coherent in the sense of the elastic matrix element. If the description of the target ground state is reliable, then such additional processes most readily enter if extra degrees of freedom are allowed for the projectile. An approach in which the projectile is treated as a Dirac particle achieves this by allowing, in addition to the positive energy to positive energy scatterings, virtual transitions to, from, and within the negative energy sector as discussed in more detail in Sec. II.

In this paper we extend the previous nonrelativistic calculations[1] to the case where the dynamics of the projectile is described by a Dirac equation.[4] We treat only the case of elastic scattering of a nucleon from a spinless nucleus. Although the Dirac equation apparently embodies the correct symmetries for such an effective one-body problem with spin $\frac{1}{2}$, the microscopic nature of the effective interaction (optical potential) is not under the same degree of theoretical control as one is accustomed to with a nonrelativistic formalism. In particular, a relativistic counterpart to standard multiple scattering expansions of the optical potential is not presently available. The separability of a Schrödinger Hamiltonian into components describing the free target nucleus, the free projectile, and a sum of residual interactions between the projectile and the target constituents, is the key feature which enables the construction of a nonrelativistic multiple scattering expansion in terms of the solutions of the subproblems for scattering from one, two, etc., constituents of the target. For a relativistic treatment, there is no simple counterpart to this feature. It is well known that a consistent description of a system of interacting Dirac particles necessitates a field-theoretical approach. In fact, the treatment of the vacuum, the interacting many-body nuclear ground state,[7] and the nonconservation of particles, as well as the specification of the projectile-nucleus residual interaction in terms of interactions with the nuclear constituents, all introduce difficulties not encountered in the Schrödinger theory. Principally for these reasons, a relativistic multiple scattering theory cannot be straightforwardly formulated along the lines of the nonrelativistic development. One must at this time take a heuristic approach. Initially, such efforts,[2] directed towards a first-order optical potential in a Dirac equation description of elastic proton scattering, appear to remove much of the inadequacy of the nonrelativistic predictions. The issues that are raised by efforts to reconcile this finding with the clear problems in specifying the underlying theoretical framework are important and deserve further study.

We calculate a relativistic optical potential in the impulse approximation (first-order in multiple scattering) by assuming a relativistic extension of the standard mechanism for the first-order Schrödinger optical potential. A simple ansatz is employed to prescribe a microscopic nucleon-nucleus interaction which operates in the 4×4 Dirac spin space of the projectile from knowledge of this interaction projected onto the positive-energy Dirac plane wave states. We take the latter quantity to be the first-order nonrelativistic optical potential so that our extension allows the effect of a Dirac description of just the projectile to be studied separately from the effect of relativistic components of the target state. This ansatz is very simple to apply. Mostly this is because the ansatz is designed to address questions separate from the required frame transformation of NN scattering amplitudes that is

an integral part of the related, but distinct, ansatz[8] employed in initial approaches of this type.[2] We show that the principal results of the previous relativistic approach are reproduced by numerical calculations based on the much simpler ansatz. Thus the essential ingredient of relativistic approaches lies in the enlargement of the Hilbert space to include negative energy intermediate states of the projectile. Eventually it is envisaged that the need for such an ansatz will be eliminated by dealing not with extrapolations from the physical NN scattering amplitudes, but rather with the separate positive and negative energy Dirac components of the NN t matrix predicted from a relativistic potential, as is obtained from boson exchange models.

The formulation and calculations presented here utilize an integral equation in a momentum-space representation. In this way, the Dirac positive and negative energy projectors can be dealt with simply and straightforward connections between the relativistic and nonrelativistic sectors can be maintained and studied. Target recoil effects can be included in a natural way. Nonlocalities, including those introduced by Dirac spinors, can be dealt with directly. Finally, this approach facilitates a study of the influence of certain off-shell and nonlocal effects related to the approximate treatment of the full-folding integral for the nuclear ground state matrix elements of the NN t matrix. This study is performed in a manner analogous to similar studies we have made in the nonrelativistic case.[1] Stability of the results to model dependence of nuclear densities is also examined. It is important to investigate such questions to see whether the characteristic differences (especially in spin observables) between the relativistic and nonrelativistic approaches are stable with respect to these typical ambiguities in the microscopic input.

In Sec. II, the Dirac equation in the presence of an external interaction is cast into the form of a coupled integral equation between two channels which correspond to the positive and negative energy Dirac plane-wave states for the projectile. After defining our notation and the methods we employ for handling the Dirac equation, we turn to the question of the microscopic content of the nucleon-nucleus interaction. The ansatz employed to obtain this from the first-order nonrelativistic optical potential is then described. Details concerning the relationship between this ansatz and the one employed in earlier work in this area[2,8] are discussed in the Appendix. The partial-wave decomposition of the positive and negative energy sectors of the optical potential is given in Sec. III as is the partial wave form of the Dirac integral equation. The numerical results are presented and discussed in Sec. IV. The summary is given in Sec. V.

II. THEORETICAL FRAMEWORK

A. Dirac equation with an external field

The differential form of the Dirac equation for the scattering of a spin $\frac{1}{2}$ particle of mass m from an external central field U is

$$(\not{p}-m-U\,|\,\Psi\rangle=0\ , \tag{1}$$

where $\not{p}=\gamma^\mu p_\mu=\gamma_\mu p^\mu$, $p^\mu=(E,-i\nabla)$, and $p_\mu=(E,i\nabla)$. The notation for four vectors and the gamma matrices is that of Bjorken and Drell.[9] We shall work within a static approximation in which the energy is fixed and only three-momentum can be transferred. The positive energy free state with momentum $\mathbf{k}$ and rest frame spin projection s satisfies

$$(\not{p}-m)\,|\,\mathbf{k},s(+)\rangle=0\ , \tag{2}$$

and has the coordinate-space form

$$\langle\,\mathbf{r}\,|\,\mathbf{k},s(+)\rangle=\frac{e^{i\mathbf{k}\cdot\mathbf{r}}}{(2\pi)^{3/2}}u(\mathbf{k},+)\,|\,\chi_s\rangle\ , \tag{3}$$

where $|\,\chi_s\rangle$ is a Pauli (two-component) spinor and $u(\mathbf{k},+)$ is a Dirac (four-component) spinor given by

$$u(\mathbf{k},+)=\left[\frac{E_k+m}{2E_k}\right]^{1/2}\begin{bmatrix}1\\ \dfrac{\boldsymbol{\sigma}\cdot\mathbf{k}}{E_k+m}\end{bmatrix}\ . \tag{4}$$

In Eq. (4), $E_k^2=k^2+m^2$, $\boldsymbol{\sigma}$ is the usual 2×2 Pauli spin matrix, and 1 is the 2×2 unit matrix. The corresponding negative energy solution of Eq. (2), with energy $-E_k$, is

$$\langle\,\mathbf{r}\,|\,\mathbf{k},s(-)\rangle=\frac{e^{i\mathbf{k}\cdot\mathbf{r}}}{(2\pi)^{3/2}}u(\mathbf{k},-)\,|\,\chi_s\rangle\ , \tag{5}$$

where

$$u(\mathbf{k},-)=\left[\frac{E_k+m}{2E_k}\right]^{1/2}\begin{bmatrix}\dfrac{-\boldsymbol{\sigma}\cdot\mathbf{k}}{E_k+m}\\ 1\end{bmatrix}\ . \tag{6}$$

The positive and negative energy free states relate to the particle and antiparticle degrees of freedom, respectively. The orthonormality relations for these basis states are

$$\langle\,\mathbf{k}',s'(\pm)\,|\,\mathbf{k},s(\pm)\rangle=\delta_{s's}\delta(\mathbf{k}'-\mathbf{k}) \tag{7}$$

and

$$\langle\,\mathbf{k}',s'(\pm)\,|\,\mathbf{k},s(\mp)\rangle=0\ . \tag{8}$$

Note that the adjoint state vectors in Eqs. (7) and (8) are the Hermitian adjoints, viz.,

$$\langle\,\mathbf{k}',s'(\pm)\,|\,\mathbf{r}\rangle=\langle\chi_{s'}\,|\,u(\mathbf{k},\pm)^\dagger\frac{e^{-i\mathbf{k}'\cdot\mathbf{r}}}{(2\pi)^{3/2}}\ , \tag{9}$$

rather than the Dirac adjoints which are

$$\langle\,\overline{\mathbf{k}',s'(\pm)}\,|=\langle\,\mathbf{k}',s'(\pm)\,|\,\gamma^0\ . \tag{10}$$

In terms of the basis states already introduced, the completeness relation is

$$\sum_s\int d^3k[\,|\,\mathbf{k},s(+)\rangle\langle\mathbf{k},s(+)\,|\,+\,|\,\mathbf{k},s(-)\rangle\langle\mathbf{k},s(-)\,|\,]=1\ . \tag{11}$$

From Eqs. (1) and (2), the integral equation equivalent of Eq. (1) is

$$|\,\Psi\rangle=|\,\mathbf{k},s(+)\rangle+\frac{1}{\not{p}-m+i\delta}U\,|\,\Psi\rangle\ , \tag{12}$$

which implements the outgoing spherical wave boundary

conditions with the limit $\delta \to 0+$. Subsequently, we shall not explicitly display the $i\delta$ term in the Dirac propagator. With a transition operator T defined as

$$T\,|\,\mathbf{k},s(+)\rangle = U\,|\,\Psi\rangle\ , \tag{13}$$

Eq. (12) leads to the operator integral equation

$$T = U + U\frac{1}{\not p - m}T\ , \tag{14}$$

which is completely equivalent to the differential form of the Dirac equation [Eq. (1)]. To make contact with a more standard notation, we introduce an operator $\widetilde{T}$ such that

$$\widetilde{T} = \gamma^0 T\ . \tag{15}$$

The physical transition matrix elements are given by

$$\begin{aligned} T_{s's}^{++}(\mathbf{k}',\mathbf{k}) &= \langle \mathbf{k}',s'(+)\,|\,\widetilde{T}\,|\,\mathbf{k},s(+)\rangle \\ &= \langle \overline{\mathbf{k}',s'(+)}\,|\,T\,|\,\mathbf{k},s(+)\rangle \\ &= \langle \chi_{s'}\,|\,T^{++}(\mathbf{k}',\mathbf{k})\,|\,\chi_s\rangle\ , \end{aligned} \tag{16}$$

where

$$\begin{aligned} T^{++}(\mathbf{k}',\mathbf{k}) &= \langle \overline{\mathbf{k}',+}\,|\,T\,|\,\mathbf{k},+\rangle \\ &= \langle \mathbf{k}',+\,|\,\widetilde{T}\,|\,\mathbf{k},+\rangle\ . \end{aligned} \tag{17}$$

Here, for convenience, we have removed the Pauli spinors to produce basis vectors $|\,\mathbf{k},\pm\rangle$, such that

$$|\,\mathbf{k},s(\pm)\rangle \equiv |\,\mathbf{k},\pm\rangle\,|\,\chi_s\rangle \tag{18}$$

and

$$\langle \overline{\mathbf{k},\pm}\,| = \langle \mathbf{k},\pm\,|\,\gamma^0\ . \tag{19}$$

The convenient quantity to deal with is $T^{++}(\mathbf{k}',\mathbf{k})$ which, as given by Eq. (17), is an operator in Pauli spin space. To make the integral equation [Eq. (14)] more explicit, the Dirac propagator can be expanded as ($\boldsymbol{\alpha} = \gamma^0\boldsymbol{\gamma}$)

$$\begin{aligned} (\not p - m)^{-1}\gamma^0 &= (E - \boldsymbol{\alpha}\cdot\mathbf{p} - \gamma^0 m)^{-1} \\ &= \int d^3k \left[\frac{|\,\mathbf{k},+\rangle\langle \mathbf{k},+\,|}{E - E_k} \right. \\ &\quad \left. + \frac{|\,\mathbf{k},-\rangle\langle \mathbf{k},-\,|}{E + E_k} \right], \end{aligned} \tag{20}$$

or

$$(\not p - m)^{-1} = \int d^3k \left[\frac{|\,\mathbf{k},+\rangle\langle \overline{\mathbf{k},+}\,|}{E - E_k} + \frac{|\,\mathbf{k},-\rangle\langle \overline{\mathbf{k},-}\,|}{E + E_k} \right]. \tag{21}$$

When Eq. (21) is employed in Eq. (14), and matrix elements are taken with respect to the same complete basis, the resulting coupled pair of integral equations can be written in the form

$$T^{++}(\mathbf{k}',\mathbf{k}) = U^{++}(\mathbf{k}',\mathbf{k}) + \int d^3k'' U^{++}(\mathbf{k}',\mathbf{k}'')\Gamma_+(k'')T^{++}(\mathbf{k}'',\mathbf{k}) + \int d^3k'' U^{+-}(\mathbf{k}',\mathbf{k}'')\Gamma_-(k'')T^{-+}(\mathbf{k}'',\mathbf{k})\ , \tag{22}$$

$$T^{-+}(\mathbf{k}',\mathbf{k}) = U^{-+}(\mathbf{k}',\mathbf{k}) + \int d^3k'' U^{-+}(\mathbf{k}',\mathbf{k}'')\Gamma_+(k'')T^{++}(\mathbf{k}'',\mathbf{k}) + \int d^3k'' U^{--}(\mathbf{k}',\mathbf{k}'')\Gamma_-(k'')T^{-+}(\mathbf{k}'',\mathbf{k})\ , \tag{23}$$

where

$$\Gamma_\pm(k'') = \frac{1}{E \mp E_{k''}}\ . \tag{24}$$

The projected interactions are

$$U^{ab}(\mathbf{k}',\mathbf{k}) = \langle \overline{\mathbf{k}',a}\,|\,U\,|\,\mathbf{k},b\rangle\ , \tag{25}$$

where a and b can stand for either of the labels $+$ or $-$. The various quantities $T(\mathbf{k}',\mathbf{k})$ and $U(\mathbf{k}',\mathbf{k})$ in Eqs. (22) and (23) are operators in Pauli spin space (2×2 matrices) and the pair of coupled equations, Eqs. (22) and (23), are just another version of the four-component Dirac equation, Eq. (1). The wave function solution of the Dirac equation may also be obtained straightforwardly from the solution of Eqs. (22) and (23) by using Eqs. (12) and (13). The relationship is

$$|\,\Psi\rangle = |\,\psi\rangle\,|\,\chi_s\rangle\ , \tag{26}$$

where

$$|\,\psi\rangle = |\,\mathbf{k},+\rangle + \frac{1}{\not p - m}T\,|\,\mathbf{k},+\rangle\ . \tag{27}$$

In terms of the basis states $|\,\mathbf{k}',\pm\rangle$, we have the expansion of the four-component Dirac state in the form

$$|\,\psi\rangle = \int d^3k' [\,|\,\mathbf{k}',+\rangle\psi_+(\mathbf{k}') + |\,\mathbf{k}',-\rangle\psi_-(\mathbf{k}')]\ , \tag{28}$$

where the projected quantities $\psi_\pm$ operate in Pauli spin space and are given by

$$\psi_+(\mathbf{k}') = \delta(\mathbf{k}' - \mathbf{k}) + \frac{1}{E - E_{k'}}T^{++}(\mathbf{k}',\mathbf{k}) \tag{29}$$

and

$$\psi_-(\mathbf{k}') = \frac{1}{E + E_{k'}}T^{-+}(\mathbf{k}',\mathbf{k})\ . \tag{30}$$

The pole in the propagator of Eq. (29) produces the outgoing wave term in the position space representation $\psi_+(\mathbf{r})$. The negative energy plane wave projection ψ_- has, of course, no incident piece and, within the present static treatment, no outgoing wave even above production threshold.

With the basis employed here, the scattering state can be represented by the column

$$|\,\psi\rangle = \begin{bmatrix} \psi_+ \\ \psi_- \end{bmatrix} |\,\chi_s\rangle\ . \tag{31}$$

This representation is *not* the same as the more usual representation in terms of "upper" and "lower" com-

ponents. The essential relativistic feature of the Dirac equation is the enlarged Hilbert space due to the appearance of the antiparticle degree of freedom on an equal footing with the particle degree of freedom. If one were to truncate the formalism so that only the particle degree of freedom were allowed, then in Eqs. (22) and (23) we would have $\Gamma_-=0$ and, thus, $\psi_-=0$. It is therefore natural to interpret ψ_+ in Eq. (31) as the "nonrelativistic" component. We note that, within the same truncation, the pair of equations that determine T^{++}, namely Eqs. (22) and (23), become simply the usual Lippmann-Schwinger equation (with relativistic kinematics), viz.,

$$T^{++}(\mathbf{k}',\mathbf{k})= U^{++}(\mathbf{k}',\mathbf{k}) + \int d^3k'' \frac{U^{++}(\mathbf{k}',\mathbf{k}'')T^{++}(\mathbf{k}'',\mathbf{k})}{E-E_{k''}} . \quad (32)$$

The interpretation of ψ_+ as the nonrelativistic sector of the wave function is suggested by the form of Eqs. (22) and (23) and Eqs. (29) and (30), and by the interpretation of the basis states $|\mathbf{k}',\pm\rangle$. We note that $\psi_+(\mathbf{k})$ is, as may be seen from Eq. (28), the probability amplitude for the system to be in the basis state $|\mathbf{k},+\rangle$ which, in turn, is a four-component object having the content of a nonrelativistic free state *only* in the rest frame. In general, the question of the identification of the nonrelativistic sector of the relativistic scattering equation is ambiguous without a specification of the interaction part of the Hamiltonian in each formulation. The microscopic description of an optical potential in first order of multiple scattering introduces two-body scattering amplitudes which, on shell at least, are determined by two-body data. This provides a strong (but incomplete) link between relativistic and nonrelativistic representations which reinforces the interpretation already discussed.

B. Microscopic approach

We recall that the first-order optical potential in the Kerman-McManus-Thaler (KMT) nonrelativistic multiple scattering theory[10] is

$$U_{\rm NR}(\mathbf{k}',\mathbf{k})=(A-1)\langle\mathbf{k}'|\langle\phi_0|t|\phi_0\rangle|\mathbf{k}\rangle , \quad (33)$$

where $|\mathbf{k}\rangle$ is a Schrödinger plane wave and $|\phi_0\rangle$ is the target ground state, normalized to unity. In the absence of a clearly defined multiple scattering expansion for the relativistic many-body problem, it is natural to seek a relativistic extension of this first-order mechanism for use in the Dirac equation. For reasons discussed in the Introduction, we shall, for this present work, retain a nonrelativistic treatment of the target ground state, and consider the effects of negative energy intermediate states and propagation for the projectile alone. The physical picture associated with Eq. (33) is that the projectile interacts with one target nucleon at a time via the NN transition operator t. The NN matrix element of t that enters represents the sum of all possible two-body interactions that can connect the initial and final asymptotic states. When these latter states are physically realizable, in a free NN collision, the t-matrix element is required to reproduce NN data. In a relativistic description, one would describe the same NN matrix element by means of a different operator, t_D, and different basis states for the particles. These basis states would be the positive energy Dirac spinors $|k,s(+)\rangle$. Accordingly, we may write

$$\langle\mathbf{k}'|\langle\mathbf{p}'|t|\mathbf{p}\rangle|\mathbf{k}\rangle\equiv\langle\overline{\mathbf{k}',+}|\langle\overline{\mathbf{p}',+}|t_D|\mathbf{p},+\rangle|\mathbf{k},+\rangle , \quad (34)$$

and with the attitude that the momentum components of $|\phi_0\rangle$ in Eq. (33) be interpreted as the amplitudes in a positive energy Dirac plane-wave expansion of the target state, we are led to adopt the identification

$$U^{++}(\mathbf{k}',\mathbf{k})=U_{\rm NR}(\mathbf{k}',\mathbf{k}) . \quad (35)$$

We must now specify the other (purely relativistic) components (U^{+-}, U^{-+}, and U^{--}) of the Dirac optical potential. We stress at this point that if the relativistic NN operator t_D, which can be defined with respect to the *full* Dirac plane wave basis (positive and negative energy), were available, then the natural extension of the NRIA is to use the right-hand side of Eq. (33) with t replaced by t_D, the Schrödinger plane waves replaced by Dirac (+ or −) plane waves, and $|\phi_0\rangle$ replaced by a suitable relativistic state. However, the operator t_D is not uniquely specified by Eq. (34). Many possible choices of t_D can satisfy Eq. (34) and reproduce the given Pauli matrix element on the left-hand side. Initial microscopic calculations[2,8] were implemented by making an ansatz for t_D that is as local as possible while having sufficient gamma matrix structure so as to reproduce the various on-shell NN Wolfenstein scattering amplitudes through Eq. (34). The matrix elements of this t_D that involve one or more negative energy Dirac plane waves were then assumed to provide a reasonable extension into the orthogonal negative energy sector of the space. The accuracy of this procedure is not known at this time and such information must await a more fundamental approach such as may be provided by the solution of a Bethe-Salpeter equation with an elementary boson exchange model for the NN force.[11] Work along these lines is in progress[12] and is beyond the scope of this paper.

In this paper we show that a very simple ansatz for the relativistic extension to the negative energy sector can reveal significant insight into the important features of the Dirac description of elastic scattering. With the identification

$$U^{++}(\mathbf{k}',\mathbf{k})=U_{\rm NR}(\mathbf{k}',\mathbf{k}) ,$$

and an optimum factorization treatment[1] of the matrix element in Eq. (33), we can write

$$U^{++}(\mathbf{k}',\mathbf{k})=U^c(\mathbf{k}',\mathbf{k})+\frac{i}{2}\boldsymbol{\sigma}\cdot\mathbf{k}'\times\mathbf{k}U^{LS}(\mathbf{k}',\mathbf{k}) , \quad (36)$$

where

$$U^c(\mathbf{k}',\mathbf{k})=\frac{A-1}{A}\eta(\mathbf{k}',\mathbf{k})t^c(\mathbf{q},\mathbf{K})\rho(q) , \quad (37)$$

and

$$U^{LS}(\mathbf{k}',\mathbf{k})=\frac{A-1}{A}\eta(\mathbf{k}',\mathbf{k})\left[\frac{A+1}{2A}\right]t^{LS}(\mathbf{q},\mathbf{K})\rho(q) . \quad (38)$$

Here $\mathbf{K}=(\mathbf{k}'+\mathbf{k})/2$ and η is the Möller factor which implements the transformation of an on-shell NN t-matrix element from the NN center of momentum frame to the N-nucleus center of momentum frame. The point nucleon density $\rho(q)$ is normalized so that $\rho(q=0)$ is the number of particles. The quantities t^c and t^{LS} are the components of the NN t matrix that survive the summations over the spin coordinates of the constituents of the target, which we take to be spin saturated. We now change to a Dirac representation by writing

$$U^{++}(\mathbf{k}',\mathbf{k})=\langle \overline{\mathbf{k}',+} \mid S+\gamma^0 V \mid \mathbf{k},+ \rangle \ , \tag{39}$$

where S is a Lorentz scalar, and V is the timelike component of a Lorentz four-vector which together describe the N-nucleus interaction U^{++}. The ansatz we employ is that the S and V derived from the *forced equality* of the representation in Eqs. (36) and (39) are to be used to calculate the extensions U^{+-}, U^{-+}, and U^{--}. That is, we take

$$U^{ab}(\mathbf{k}',\mathbf{k})=\langle \overline{\mathbf{k}',a} \mid S+\gamma^0 V \mid \mathbf{k},b \rangle \ , \tag{40}$$

where a and b can each be either $+$ or $-$. This is similar in spirit to the prescription[2,8] that a postulated Lorentz invariant content of t^{++} can be used to generate t^{+-}, t^{-+}, and t^{--}, except that the application here is made at the level of the optical potential rather than at the NN t-matrix level. Equations (36)—(40) define the Dirac optical potential which is employed in the present work together with the integral Eqs. (22) and (23) to calculate scattering observables. This procedure is equivalent to setting $U=S+\gamma^0 V$ in the Dirac differential equation given by Eq. (1).[13]

We note that any microscopic treatment will give to $U^{++}(\mathbf{k}',\mathbf{k})$ the structure displayed in Eq. (36) due to invariance arguments linked to the spin $\frac{1}{2}\otimes$ spin 0 structure of the problem. The extension ansatz embodied by Eqs. (39) and (40) does not rely upon detailed knowledge of the microscopic content of U^c and U^{LS}. The expression for U^c and U^{LS} in terms of NN scattering operators and nuclear densities will vary with the type of microscopic approach. We have chosen to employ expressions for U^c and U^{LS} that come directly from a nonrelativistic approach. The implications that our approach has for treatments of the Lorentz transformation properties of NN scattering operators and for relativistic components of nuclear densities are discussed in the Appendix. We also note that at this level of treatment there is no fundamental reason for choosing the Lorentz structure $S+\gamma^0 V$ in Eq. (39). There are many other Lorentz structures with different momentum and gamma matrix dependence that could be used in Eq. (39) while still reproducing the form given in Eq. (36).[14] For example, a Lorentz tensor could be used in place of either the scalar or vector. The results for U^{+-}, U^{-+}, and U^{--} would then, in general, be different. This ambiguity is tied to the problem of obtaining a unique determination of the Lorentz structure of the NN scattering operator, as discussed earlier. Even if that problem were under reasonable control, there is still considerable ambiguity as to whether a more fundamental approach from a field theory would justify a multiple scattering structure of the same *form* as the nonrelativistic one. In the absence of a fundamental approach, we choose $S+\gamma^0 V$ as already indicated for simplicity and for comparison with both phenomenological analysis of scattering[15] and mean-field treatments of nuclear ground states.[16]

An aspect of the nonrelativistic KMT multiple scattering structure that does retain its meaning in the relativistic circumstance is the weighting factor of $A-1$ (rather than A) in Eq. (33). A consideration of the implications of this factor leads to an interesting insight into the physical picture associated with a first-order relativistic optical potential, in contrast to that in the nonrelativistic case. To discuss the point, we consider that the relativistic optical potential is described by

$$U^{ab}(\mathbf{k}',\mathbf{k})=(A-1)\langle \overline{\mathbf{k}',a} \mid \langle \bar{\psi}_0 \mid t_D \mid \psi_0 \rangle \mid \mathbf{k},b \rangle \ , \tag{41}$$

$$=\frac{A-1}{A}\langle \overline{\mathbf{k}',a} \mid \langle \bar{\psi}_0 \mid \sum_{i=1}^{A} t_D^i \mid \psi_0 \rangle \mid \mathbf{k},b \rangle \ , \tag{42}$$

where a and b can each be $+$ or $-$, ψ_0 is a suitable relativistic description of the target ground state, and t_D is an operator in the Dirac spinor space describing the scattering of the projectile and target particle i. The integral form of the Dirac equation [Eqs. (22) and (23)], when expressed in single channel form through formal elimination of the negative energy channel, becomes[17]

$$T^{++}=W^{++}+W^{++}\Gamma_+ T^{++} \ , \tag{43}$$

where

$$W^{++}=U^{++}+U^{+-}\frac{1}{\Gamma_-^{-1}-U^{--}}U^{-+} \ . \tag{44}$$

The physical scattering operator $\mathscr{T}^{++}$ is related to the KMT operator T^{++} through $\mathscr{T}^{++}=(A/A-1)T^{++}$. Thus, $\mathscr{T}^{++}$ satisfies

$$\mathscr{T}^{++}=\mathscr{W}^{++}+\left[\frac{A-1}{A}\right]\mathscr{W}^{++}\Gamma_+\mathscr{T}^{++} \ , \tag{45}$$

where $\mathscr{W}^{++}=(A/A-1)W^{++}$. With retention of only the first-order effect of the coupling to the negative energy states in Eq. (44) (that is, $U^{--}=0$), the operator $\mathscr{W}^{++}$ in the projectile space can be expressed as

$$\mathscr{W}^{++}\approx\sum_{i=1}^{A}\langle \bar{\psi}_0 \mid t_D^i \mid \psi_0 \rangle + \sum_{i\neq j}^{A}\langle \bar{\psi}_0 \mid t_D^i \mid \psi_0 \rangle \mathscr{G}_-\langle \bar{\psi}_0 \mid t_D^j \mid \psi_0 \rangle \ , \tag{46}$$

where

$$\mathscr{G}_-=\int d^3k \mid \mathbf{k},- \rangle \Gamma_-(k) \langle \overline{\mathbf{k},-} \mid \ . \tag{47}$$

The second term of Eq. (46) is the leading term of the relativistic modification arising from treating the projectile as a Dirac particle. If only the first term in Eq. (46) is retained, then the treatment of the projectile is nonrelativistic. In nonrelativistic multiple scattering theory,[10] terms of higher order than this necessarily involve an excitation of the target via the projectile scattering from one target nucleon, a propagation of this excited system, and

then a deexcitation of the target as the projectile scatters from a *different* target nucleon. Thus a target correlation density is involved. However, in the relativistic description of the projectile, terms involving scattering of the projectile from two (or more) distinct nucleons of the target can enter without being coupled to target correlation effects, viz., the second term of Eq. (46) in which the target always remains in its ground state. This is a direct consequence of the enlargement of the Hilbert space available to the projectile. The second term of Eq. (46) corresponds to the process often referred to as the Z graph in field theory. Because of the static treatment of the present formulation, the negative energy plane-wave intermediate states do not have as close an association with antinucleons as would be possible in a truly covariant description of the dynamics.

III. PARTIAL WAVE PROJECTIONS OF THE INTERACTIONS AND THE INTEGRAL EQUATION

The Dirac momentum-space integral equations [Eqs. (22) and (23)] are to be solved separately for each angular momentum state. The particularly simple form of these equations is due to the fact that each of the quantities T^{++}, T^{-+}, U^{++}, U^{+-}, U^{-+}, and U^{--} is an operator in the two-dimensional Pauli spin space. Here we outline the expansion of these quantities in (Pauli) spinor-spherical harmonics, and derive the resulting projected form of the integral equations. We discuss the techniques in some detail because they yield additional insight into the structure of the coupling between the positive and negative energy spaces, and because the nature of some of the expansions is somewhat different from what is encountered in Schrödinger-type treatments. We first give the explicit forms for the four components U^{++}, U^{+-}, U^{-+}, and U^{--} of the Dirac optical potential employed here. From Eq. (40), with the notation $U=S+\gamma^0 V$, we find

$$U^{++}(\mathbf{k}',\mathbf{k})=\langle\overline{\mathbf{k}',+}\,|\,U\,|\,\mathbf{k},+\rangle = N_{k'}N_k\left[(V+S)+\frac{(V-S)}{\epsilon_{k'}\epsilon_k}\times(\mathbf{k}'\cdot\mathbf{k}+i\boldsymbol{\sigma}\cdot\mathbf{k}'\times\mathbf{k})\right], \tag{48}$$

where

$$\epsilon_k=E_k+m=(k^2+m^2)^{1/2}+m\ , \tag{49}$$

and from Eq. (4) the normalization constant of the Dirac spinors is

$$N_k=\left[\frac{\epsilon_k}{2E_k}\right]^{1/2}. \tag{50}$$

For convenience, we denote $V(\mathbf{k}',\mathbf{k})$ and $S(\mathbf{k}',\mathbf{k})$ by simply V and S. We can explicitly see at this stage the identity in form between Eqs. (36) and (48). In like manner, Eq. (40) also yields

$$U^{+-}(\mathbf{k}',\mathbf{k})=\langle\overline{\mathbf{k}',+}\,|\,U\,|\,\mathbf{k},-\rangle = N_{k'}N_k\left[\frac{\boldsymbol{\sigma}\cdot\mathbf{k}'}{\epsilon_{k'}}(V-S)-(V+S)\frac{\boldsymbol{\sigma}\cdot\mathbf{k}}{\epsilon_k}\right], \tag{51}$$

$$U^{-+}(\mathbf{k}',\mathbf{k})=\langle\overline{\mathbf{k}',-}\,|\,U\,|\,\mathbf{k},+\rangle = N_{k'}N_k\left[(V-S)\frac{\boldsymbol{\sigma}\cdot\mathbf{k}}{\epsilon_k}-\frac{\boldsymbol{\sigma}\cdot\mathbf{k}'}{\epsilon_{k'}}(V+S)\right], \tag{52}$$

and

$$U^{--}(\mathbf{k}',\mathbf{k})=\langle\overline{\mathbf{k}',-}\,|\,U\,|\,\mathbf{k},-\rangle = N_{k'}N_k\left[(V-S)+\frac{(V+S)}{\epsilon_{k'}\epsilon_k}\times(\mathbf{k}'\cdot\mathbf{k}+i\boldsymbol{\sigma}\cdot\mathbf{k}'\times\mathbf{k})\right]. \tag{53}$$

It is useful to define the auxiliary quantities D and F, such that

$$D(\mathbf{k}',\mathbf{k})=N_{k'}N_k[V(\mathbf{k}',\mathbf{k})-S(\mathbf{k}',\mathbf{k})] \tag{54}$$

and

$$F(\mathbf{k}',\mathbf{k})=N_{k'}N_k[V(\mathbf{k}',\mathbf{k})+S(\mathbf{k}',\mathbf{k})]\ , \tag{55}$$

since these are the only combinations that appear. Given the nonrelativistic optical potential in the form of Eq. (36), our ansatz for determining V and S can now be expressed as

$$D(\mathbf{k}',\mathbf{k})=\frac{\epsilon_{k'}\epsilon_k}{2}U^{LS}(\mathbf{k}',\mathbf{k})\ , \tag{56}$$

and

$$F(\mathbf{k}',\mathbf{k})=U^c(\mathbf{k}',\mathbf{k})-\tfrac{1}{2}\mathbf{k}'\cdot\mathbf{k}U^{LS}(\mathbf{k}',\mathbf{k})\ . \tag{57}$$

We introduce the angular momentum expansion for the rotational invariant $F(\mathbf{k}',\mathbf{k})$ as

$$F(\mathbf{k}',\mathbf{k})=4\pi\sum_{JLM}\mathscr{Y}^M_{JL}(\hat{\mathbf{k}}')F_L(k',k)\mathscr{Y}^{M\dagger}_{JL}(\hat{\mathbf{k}})\ , \tag{58}$$

$$=4\pi\sum_{LM_L}Y_L^{M_L}(\hat{\mathbf{k}}')F_L(k',k)Y_L^{M_L^*}(\hat{\mathbf{k}})\ , \tag{59}$$

along with a similar expansion for D, U^c, and U^{LS}. Here, $\mathscr{Y}^M_{JL}(\hat{\mathbf{k}})$ is the standard (Pauli) spinor-spherical harmonic defined by

$$\mathscr{Y}^M_{JL}(\hat{\mathbf{k}})=\sum_{M_L,s}Y_L^{M_L}(\hat{\mathbf{k}})\,|\,\chi_s\rangle\langle LM_L;\tfrac{1}{2}s\,|\,JM\rangle \tag{60}$$

in terms of spherical harmonics and Clebsch-Gordan coefficients. The angular momentum projected form of Eqs. (56) and (57) is easily seen to be

$$D_L(k',k)=\frac{\epsilon_{k'}\epsilon_k}{2}U_L^{LS}(k',k) \tag{61}$$

and

$$F_L(k',k)=U_L^{\epsilon}(k',k)-\frac{k'k}{2(2L+1)}\times[(L+1)U_{L+1}^{LS}+LU_{L-1}^{LS}]\ . \tag{62}$$

For a given D and F, the full Dirac optical potential can be expressed as

$$U^{++}(\mathbf{k}',\mathbf{k})=F(\mathbf{k}',\mathbf{k})+\frac{D(\mathbf{k}',\mathbf{k})}{\epsilon_{k'}\epsilon_k}\times(\mathbf{k}'\cdot\mathbf{k}+i\boldsymbol{\sigma}\cdot\mathbf{k}'\times\mathbf{k})\ , \tag{63}$$

$$U^{+-}(\mathbf{k}',\mathbf{k})=\frac{\boldsymbol{\sigma}\cdot\mathbf{k}'}{\epsilon_{k'}}D(\mathbf{k}',\mathbf{k})-F(\mathbf{k}',\mathbf{k})\frac{\boldsymbol{\sigma}\cdot\mathbf{k}}{\epsilon_k}\ , \tag{64}$$

$$U^{-+}(\mathbf{k}',\mathbf{k})=D(\mathbf{k}',\mathbf{k})\frac{\boldsymbol{\sigma}\cdot\mathbf{k}}{\epsilon_k}-\frac{\boldsymbol{\sigma}\cdot\mathbf{k}'}{\epsilon_{k'}}F(\mathbf{k}',\mathbf{k})\ , \tag{65}$$

and

$$U^{--}(\mathbf{k}',\mathbf{k})=D(\mathbf{k}',\mathbf{k})+\frac{F(\mathbf{k}',\mathbf{k})}{\epsilon_{k'}\epsilon_k}(\mathbf{k}'\cdot\mathbf{k}+i\boldsymbol{\sigma}\cdot\mathbf{k}'\times\mathbf{k})\ . \tag{66}$$

We now require the angular momentum expansions of these quantities. There are only two types of expansion required because when the roles of F and D are reversed, U^{++} becomes U^{--}, and when the roles of F and $-D$ are reversed, U^{+-} becomes U^{-+}. The expansion of U^{++} is of the standard form encountered in momentum-space treatments of nonrelativistic optical potentials.[1] The result is

$$U^{++}(\mathbf{k}',\mathbf{k})=4\pi\sum_{JLM}\mathscr{Y}_{JL}^{M}(\hat{\mathbf{k}}')U_{JL}^{++}(k',k)\mathscr{Y}_{JL}^{M\dagger}(\hat{\mathbf{k}})\ , \tag{67}$$

with

$$U_{JL}^{++}(k',k)=F_L(k',k)+\frac{k'k}{\epsilon_{k'}\epsilon_k}D_{\bar{L}}(k',k)\ , \tag{68}$$

where $\bar{L}=2J-L$.

The optical potentials U^{+-} and U^{-+}, which link the positive and negative energy sectors of the Dirac space, are pseudoscalar because of the $\boldsymbol{\sigma}\cdot\mathbf{k}$ and $\boldsymbol{\sigma}\cdot\mathbf{k}'$ factors occurring in Eqs. (64) and (65), and hence do not conserve parity. The angular momentum expansion of these potentials will be purely off diagonal in orbital angular momentum, but still diagonal in total angular momentum. The expansion can be derived by initially considering the first term of Eq. (64). From the expansion

$$D(\mathbf{k}',\mathbf{k})=4\pi\sum_{JLM}\mathscr{Y}_{JL}^{M}(\hat{\mathbf{k}}')D_L(k',k)\mathscr{Y}_{JL}^{M\dagger}(\hat{\mathbf{k}})\ , \tag{69}$$

and the identity

$$\boldsymbol{\sigma}\cdot\hat{\mathbf{k}}'\mathscr{Y}_{JL}^{M}(\hat{\mathbf{k}}')=-\mathscr{Y}_{J\bar{L}}^{M}(\hat{\mathbf{k}}')\ , \tag{70}$$

which follows from the fact that $\boldsymbol{\sigma}\cdot\hat{\mathbf{k}}'$ is a Hermitian, unitary, pseudoscalar operator that commutes with J^2 and J_z, we have that

$$\boldsymbol{\sigma}\cdot\hat{\mathbf{k}}'D(\mathbf{k}',\mathbf{k})=-4\pi\sum_{JLM}\mathscr{Y}_{J\bar{L}}^{M}(\hat{\mathbf{k}}')D_L(k',k)\mathscr{Y}_{JL}^{M\dagger}(\hat{\mathbf{k}})\ . \tag{71}$$

In this way all four terms involved in Eqs. (64) and (65) may be expanded and the results may be expressed in the form ($\bar{L}=2J-L$)

$$U^{+-}(\mathbf{k}',\mathbf{k})=4\pi\sum_{JLM}\mathscr{Y}_{JL}^{M}(\hat{\mathbf{k}}')U_{JL}^{+-}(k',k)\mathscr{Y}_{J\bar{L}}^{M\dagger}(\hat{\mathbf{k}})\ , \tag{72}$$

where

$$U_{JL}^{+-}(k',k)=F_L(k',k)\frac{k}{\epsilon_k}-\frac{k'}{\epsilon_{k'}}D_{\bar{L}}(k',k)\ , \tag{73}$$

and

$$U^{-+}(k',k)=4\pi\sum_{JLM}\mathscr{Y}_{J\bar{L}}^{M}(\hat{\mathbf{k}}')U_{JL}^{-+}(k',k)\mathscr{Y}_{JL}^{M\dagger}(\hat{\mathbf{k}})\ , \tag{74}$$

where

$$U_{JL}^{-+}(k',k)=\frac{k'}{\epsilon_{k'}}F_L(k',k)-D_{\bar{L}}(k',k)\frac{k}{\epsilon_k}\ . \tag{75}$$

We note that despite the coupling between L and $\bar{L}$ states, the angular momentum projections of U^{+-} and U^{-+} need only be labeled by J, and by a single L value which we choose for later convenience to be that of the positive energy state. The negative energy state coupled to this is uniquely specified by J and $\bar{L}=2J-L$. Because $F_L(k',k)$ and $D_L(k',k)$ are symmetric under interchange of k' and k, Eqs. (73) and (75) exhibit the important symmetry relation

$$U_{JL}^{+-}(k',k)=U_{JL}^{-+}(k,k')\ . \tag{76}$$

From Eqs. (63), (66), and (68), an interchange of the roles of F and D allows expansion of $U^{--}(\mathbf{k}',\mathbf{k})$ to be written as

$$U^{--}(\mathbf{k}',\mathbf{k})=4\pi\sum_{JLM}\mathscr{Y}_{J\bar{L}}^{M}(\hat{\mathbf{k}}')U_{JL}^{--}(k',k)\mathscr{Y}_{J\bar{L}}^{M\dagger}(\hat{\mathbf{k}})\ , \tag{77}$$

where

$$U_{JL}^{--}(k',k)=D_{\bar{L}}(k',k)+\frac{k'k}{\epsilon_{k'}\epsilon_k}F_L(k',k)\ . \tag{78}$$

Here we have labeled the component by the L value of the positive energy state that it will *eventually* be coupled to. This allows the integral equations to be expressed in a concise form.

The above-mentioned angular momentum expansion of the optical potentials, together with the coupled integral equations [Eqs. (22) and (23)] for T^{++} and T^{-+}, serve to define the corresponding expansions of these latter quantities. The most general form for the angular momentum expansions for T^{++} and T^{-+} may be adopted and the integral equations iterated using the above-mentioned optical potential expansions to confirm the following results. The expansions for T^{++} and T^{-+} are necessarily of the form

$$T^{++}(\mathbf{k}',\mathbf{k})=4\pi\sum_{JLM}\mathscr{Y}_{JL}^{M}(\hat{\mathbf{k}}')T_{JL}^{++}(k',k)\mathscr{Y}_{JL}^{M\dagger}(\hat{\mathbf{k}}) \tag{79}$$

and

$$T^{-+}(\mathbf{k}',\mathbf{k})=4\pi\sum_{JLM}\mathscr{Y}_{J\bar{L}}^{M}(\hat{\mathbf{k}}')T_{JL}^{-+}(k',k)\mathscr{Y}_{JL}^{M\dagger}(\hat{\mathbf{k}})\ . \tag{80}$$

The integral equations in partial wave form are

$$T_{JL}^{++}(k',k)=U_{JL}^{++}(k',k)+4\pi\sum_{\alpha=+,-}\int dk''k''^2U_{JL}^{+\alpha}(k',k'')\frac{1}{E-\lambda_\alpha E_{k''}}T_{JL}^{\alpha+}(k'',k) \tag{81}$$

and

$$T_{JL}^{-+}(k',k)=U_{JL}^{-+}(k',k)+4\pi\sum_{\alpha=+,-}\int dk''k''^2U_{JL}^{-\alpha}(k',k'')\frac{1}{E-\lambda_\alpha E_{k''}}T_{JL}^{\alpha+}(k'',k)\,, \tag{82}$$

where $\lambda_+=+1$, and $\lambda_-=-1$. The fact that these integral equations are diagonal in J and independent of the projection M of J is a reflection of the rotational invariance of the system. The appearance of only a single orbital angular momentum label in these equations is a consequence of our labeling scheme. The full effects associated with the lowering (or raising) of the L value by one unit via U^{-+} and the subsequent raising (or lowering) of the L value via U^{+-} are automatically included.

The results presented in Sec. IV are obtained by numerical solution of Eqs. (81) and (82) for a set of (J,L) values up to some maximum values such that the Born approximation $T^{++}\approx U^{++}$ is sufficiently accurate beyond that point. The contributions to T^{++} from *all* higher (J,L) values are obtained from an evaluation of $U^{++}(\mathbf{k}',\mathbf{k})$ via Eq. (63) followed by a subtraction of the lower angular momentum components of $U^{++}(\mathbf{k}',\mathbf{k}')$, which are included in the set of (J,L) values for which Eqs. (81) and (82) are solved. The nonrelativistic results with which we compare are obtained simply by setting U^{+-} to zero, thereby removing the coupling to negative energy states and reverting, in effect, to Eq. (32). The only input required for these calculations is the nonrelativistic optical potential. The relativistic extension ansatz that we employ here fixes all other ingredients. A more detailed description of the microscopic construction of the nonrelativistic optical potential is provided in Ref. 1.

IV. RESULTS

Some representative calculations for the elastic scattering of protons from ^{40}Ca and ^{16}O are presented in the following. These target nuclei were chosen because they are zero-spin, spin-saturated, $N=Z$ nuclei, for which the neutron and proton distributions may be considered to be almost identical. Thus, the only input to these calculations consists of the density of the target nucleus, inferred from electron scattering measurements, and the nucleon-nucleon t matrix, inferred from nucleon-nucleon scattering measurements. Any incongruities between the predictions and the elastic scattering data in this study are considered from the point of view of either failures of the theoretical assumptions or incomplete knowledge of the input quantities for the calculations.

We show calculations for the differential cross section $d\sigma/d\Omega$, the analyzing power A_y, and the spin rotation function Q. Whenever data are available, these are shown on the figures. Unless otherwise indicated, the point proton density was obtained from the nuclear charge density which was taken to be a three-parameter Fermi shape with parameters fixed at values determined by an analysis[18] of electron scattering data. The point neutron density was set equal to the point proton density.

A. Comparison of relativistic and nonrelativistic calculations

In Figs. 1–7 the scattering observables $d\sigma/d\Omega$, A_y, and Q, calculated according to the relativistic prescription

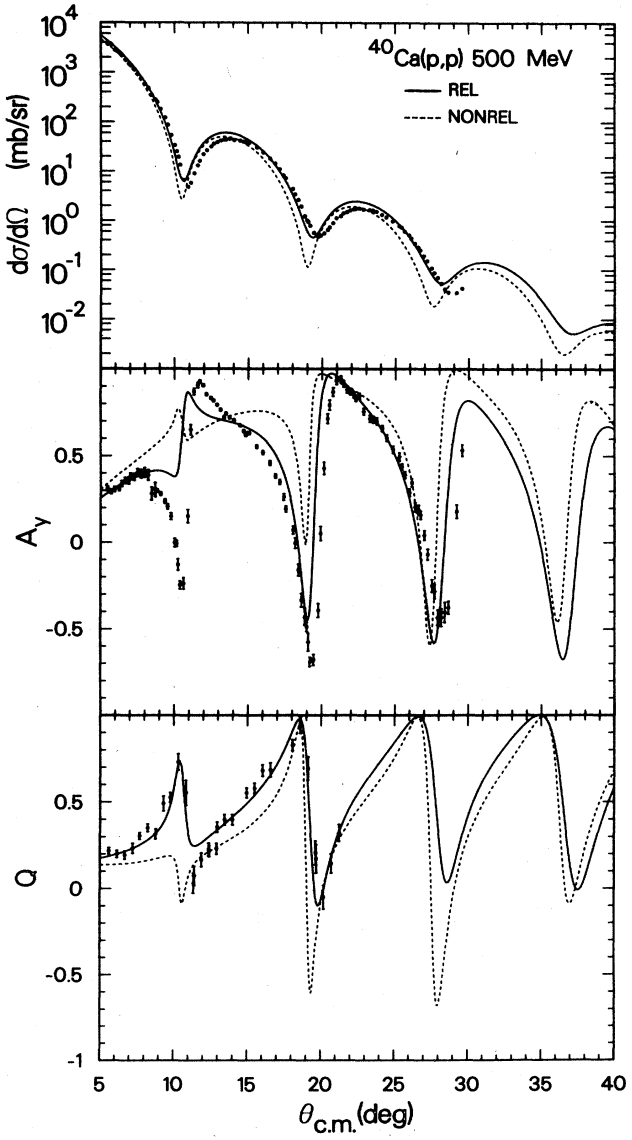

FIG. 1. Differential cross section, analyzing power, and spin rotation function for 500 MeV protons scattered from ^{40}Ca. The solid and dashed lines represent the relativistic and nonrelativistic calculations described in the text. Off shell and nonlocal effects as represented through the optimum factorization prescription are included. The data are from Ref. 24.

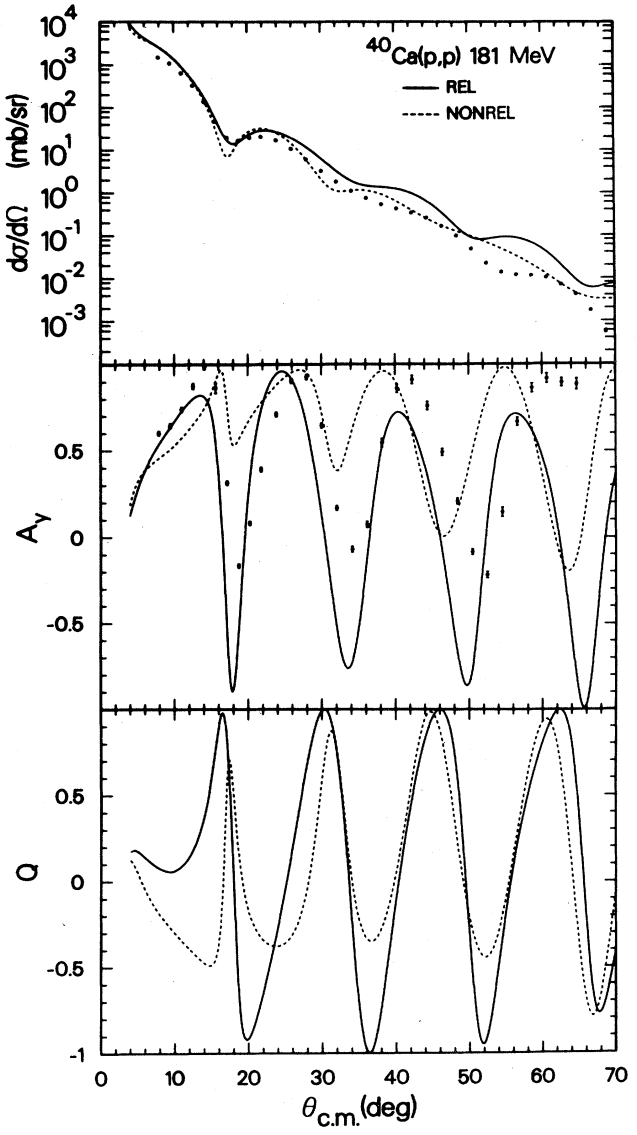

FIG. 2. Same as for Fig. 1, except the energy is 181 MeV and the data are from Ref. 25.

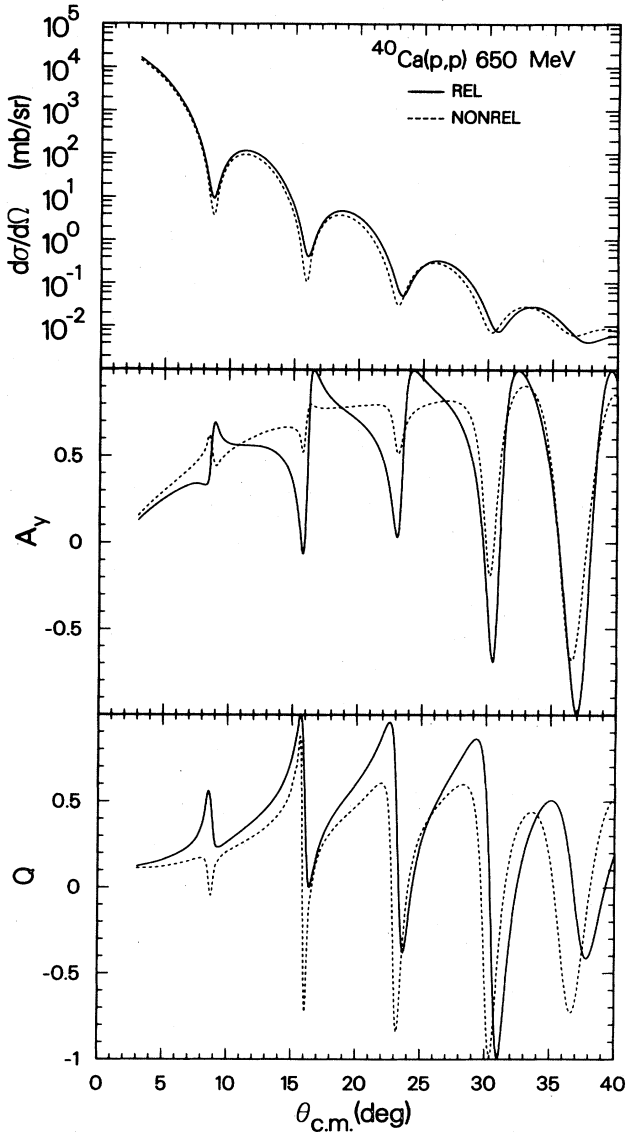

FIG. 3. Same as for Fig. 1, except the energy is 650 MeV.

described in Sec. II, are shown as solid curves. These results are compared with the related nonrelativistic calculations (dashed curves) obtained as described here and in Ref. 1. We first turn our attention to the scattering of protons from ^{40}Ca at 500 MeV. This is an ideal case against which to test the first-order nonrelativistic multiple scattering theory predictions. At higher energies, pion production presents difficulties. At lower energies, higher order terms in the multiple scattering series and residual Pauli effects may become too important to neglect. Furthermore, the charge distribution of ^{40}Ca is very well known and we have very good reason to believe that the matter distribution follows closely the point proton distribution for this nucleus. Thus any failure of the calculations to account for the data at low momentum transfer in this (most favorable) case leaves us with a theory with no regime of applicability.

In Fig. 1(a) we show the angular distribution for p-^{40}Ca elastic scattering at 500 MeV. The data is of high precision. The nonrelativistic curve (dashed) does not provide an adequate description of this data at the level we require. The diffraction pattern is pulled in as though the "size of the interaction region" was slightly too large and the minima are somewhat too sharp as though the edge of the interaction region was not quite diffuse enough. Furthermore, from the studies in Ref. 1, we conclude that the input uncertainties to the calculations do not account for the discrepancy between the theoretical curves and the data points. The relativistic (solid) curve describes the data set much more accurately. The results of the relativistic calculation give a diffraction pattern which is more spread out and whose diffraction minima are shallower, so that, all in all, the angular distribution predicted by the relativistic calculation is in good agreement with the data, both qualitatively and quantitatively.

The analyzing power A_y for ^{40}Ca at 500 MeV is shown

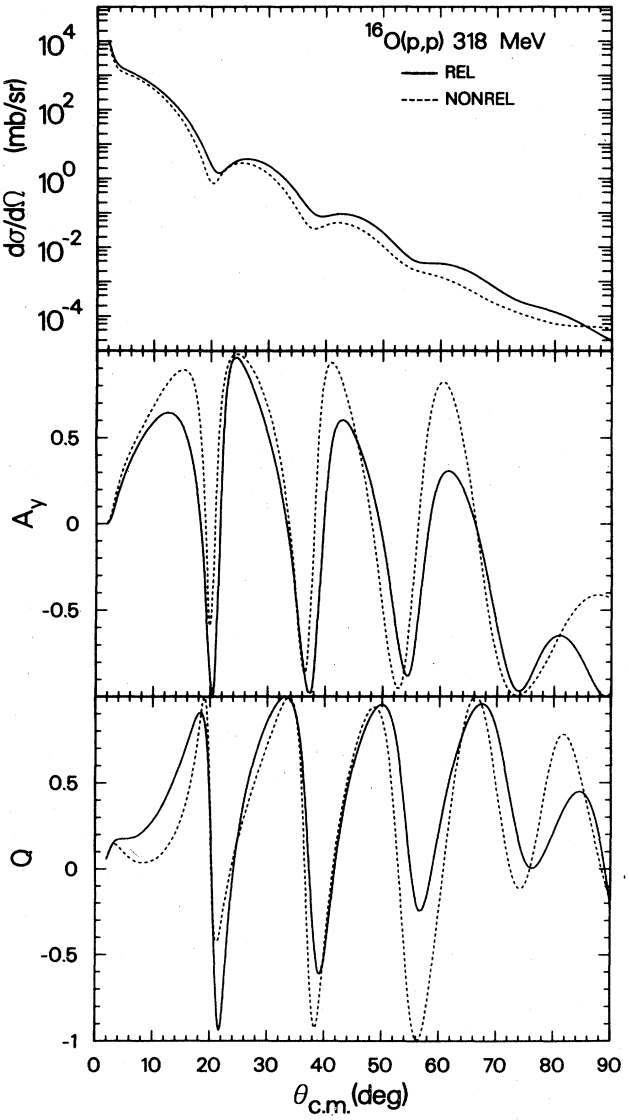

FIG. 4. Same as for Fig. 1, except for ^{16}O at an energy of 318 MeV.

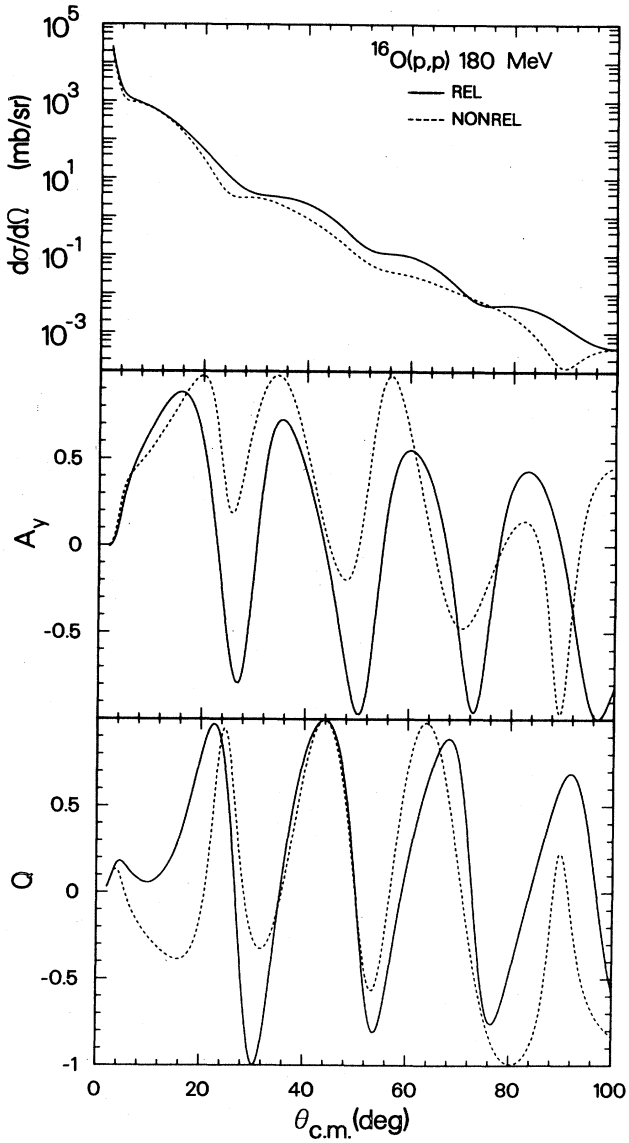

FIG. 5. Same as for Fig. 1, except for ^{16}O at an energy of 180 MeV.

in Fig. 1(b). Here we see the often quoted failure of the nonrelativistic calculations. The dashed curve rises beyond 7°, showing a peak where the data shows a deep minimum. Again at 18°, the dashed curve has a broad shoulder where the data shows a rapid decline from positive to negative polarization. The relativistic calculation, on the other hand, has none of these unsatisfactory features. There are indeed sharp dips in the 10° and 19° angular regions. Were it not for the fact that the relativistic calculation does not show a deep enough excursion to negative values in the region of the first diffraction minimum, a very accurate description of the data would be evident. Furthermore, we shall present calculations in the following which show that this particular feature of the analyzing power is extraordinarily sensitive to very small changes in the Lorentz vector-scalar composition of the optical potential, so that it is easy to get a spectacularly good description of these data, but not so easy to extract a unique physical interpretation of the changes which give rise to this improvement.

The 500 MeV ^{40}Ca spin rotation function Q is shown in Fig. 1(c). Here, again, we may sharply differentiate between the relativistic and nonrelativistic predictions. At the first diffraction minimum, the nonrelativistic result has a completely different character than the data set. The relativistic result provides a very good description except for the sharpness of the first minimum, which we shall see later on is a reflection of the same sensitivity discussed with respect to the analyzing power. Overall, if correlative and Pauli effects are indeed as small as expected in this case, the importance of relativistic effects is quite clear. These relativistic results have all of the qualitative features of the phenomenological results[15] in which the parameters of a Lorentz scalar (S) and vector (V) potential are varied to precisely fit the data. From the point of view of the ansatz used here, quite acceptable values of

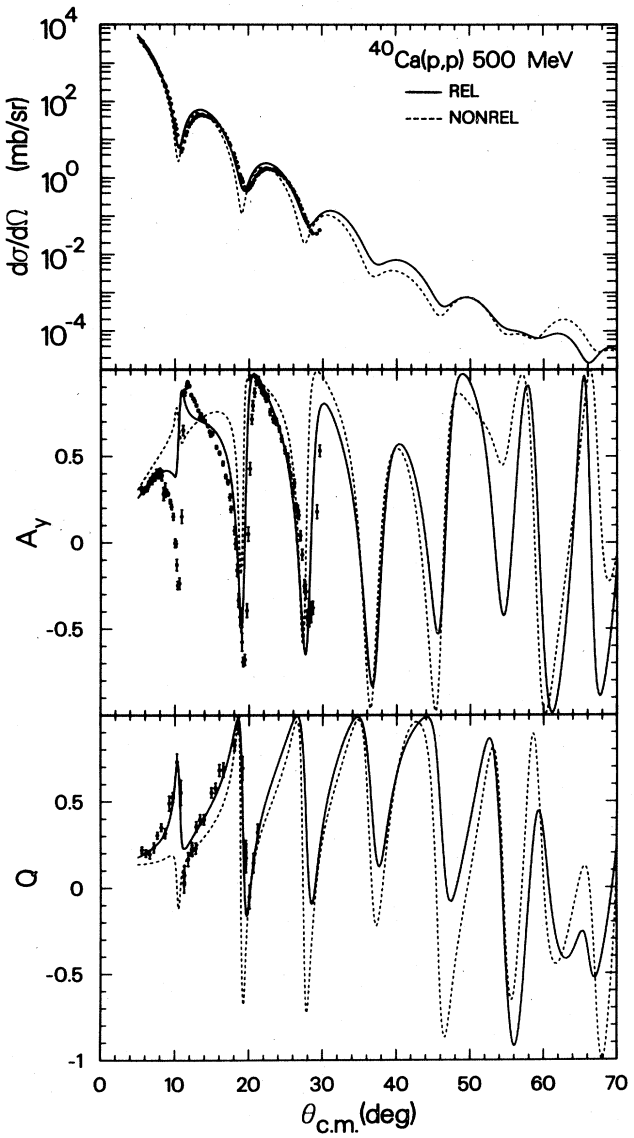

FIG. 6. Same as for Fig. 1, except that here an increased range of scattering angle is displayed.

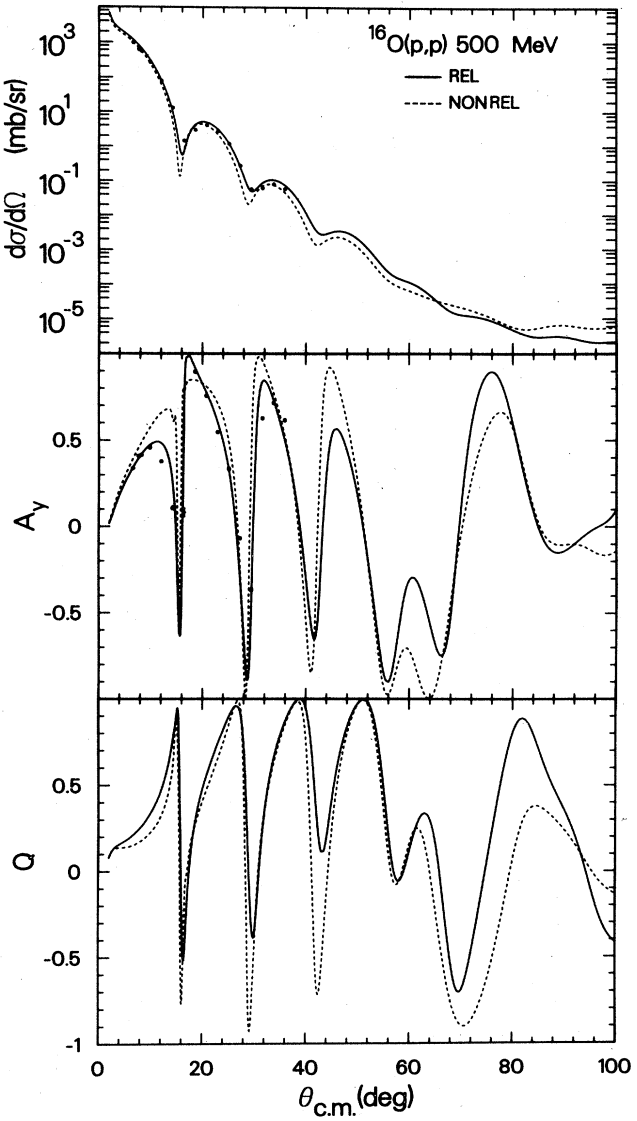

FIG. 7. Same as for Fig. 1, except for ^{16}O at an energy of 500 MeV, and the data is from Ref. 26.

S and V can be inferred from the content of a microscopic nonrelativistic optical potential. From the point of view of the relativistic extension ansatz employed in Ref. 2, values of the scalar, vector, and tensor components that produce a superior description of the data are inferred from the NN scattering amplitudes. As we will see, the results provided by these two different assumptions are much closer for other energies.

We next consider the results shown in Fig. 2 for the scattering of protons from ^{40}Ca at 181 MeV. This is too low an energy to expect *a priori* that a first-order optical potential will yield good agreement with the data. Nevertheless, the comparison of the relativistic and nonrelativistic predictions with the data can be most informative. Neither the relativistic nor the nonrelativistic curves provide a satisfactory description of the differential cross section data. The nonrelativistic prediction has the first two diffraction minima more sharply defined than may be observed in the data. The relativistic prediction is somewhat better in the vicinity of the first diffraction minimum, but lies well above the data at angles beyond 20°. The relativistic prediction thus may perhaps be judged to yield a slightly better, but in any event no worse, description of the angular distribution data than does the nonrelativistic calculation.

For the analyzing power shown in Fig. 2(b), the nonrelativistic (dashed) curve contains some similarities with the data, however the agreement is rather poor, even at small angles. The improvement provided by the relativistic calculation lies in a deepening and a shift of the minima. Of particular note is the improved behavior at small angles. A first-order multiple scattering mechanism should be most reliable there, and the adoption of a relativistic approach appears to bring this expectation closer

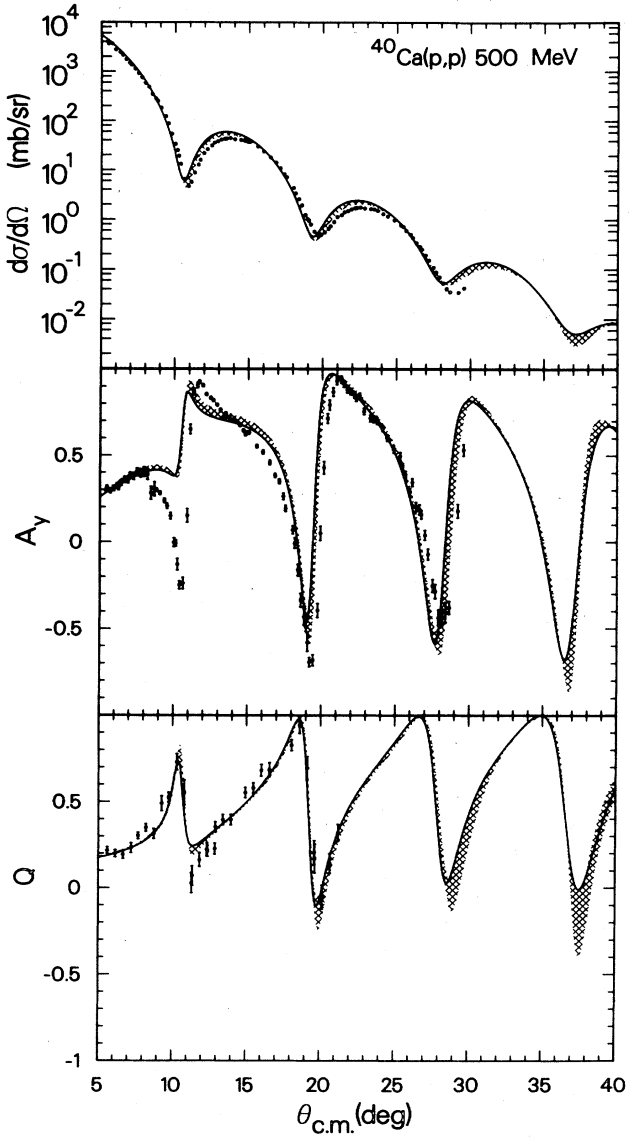

FIG. 8. Differential cross section analyzing power and spin rotation function for 500 MeV protons scattered from ^{40}Ca. The solid line corresponds to the same relativistic calculation employed for earlier figures. The cross-hatched areas represent the uncertainties due to off-shell and nonlocal effects as described in the text. The data is from Ref. 24.

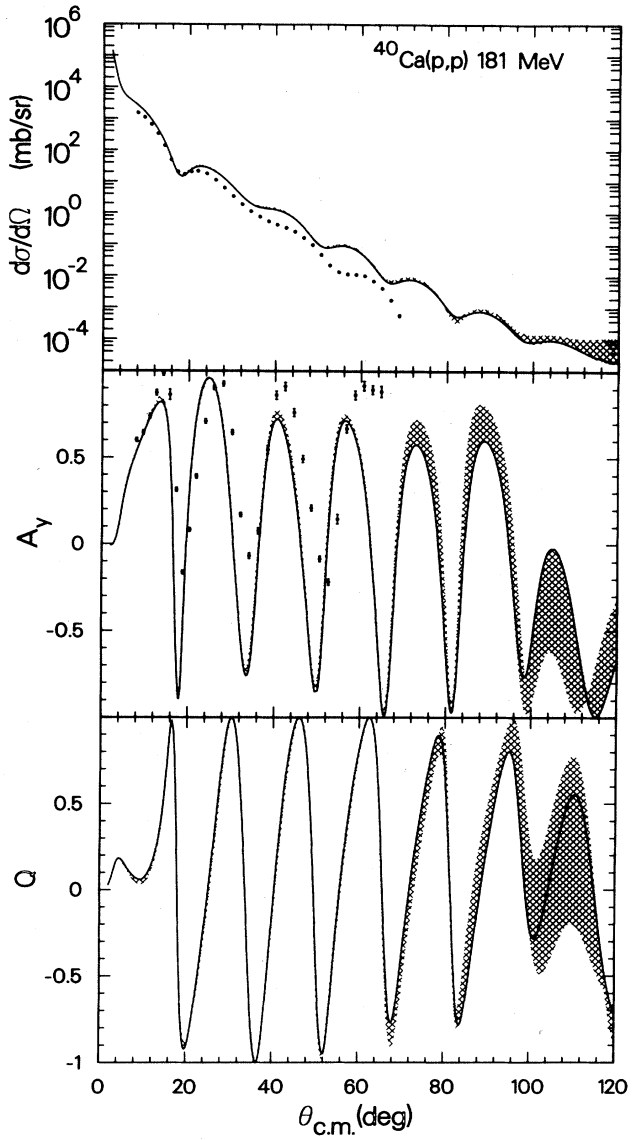

FIG. 9. Same as for Fig. 8, except that the energy is 181 MeV and the data are from Ref. 25.

to fulfillment than would be deduced from a nonrelativistic approach.

The spin rotation function for ^{40}Ca at 181 MeV is shown in Fig. 2(c). There are no data presently available for Q at this energy. We may observe that the qualitative difference between the two curves for A_y in the 10°—20° region is reflected in a large qualitative difference in that same regime for Q. At larger angles, the main relativistic effect is a deepening of the minima.

In this energy range, calculations which use a medium-modified NN t matrix within a nonrelativistic first-order optical potential approach also produce a deepening of the minima in A_y similar to the data.[19] The common element between such an approach and the relativistic approach followed here is a nonlinear dependence of the optical potential upon the nuclear density. Terms beyond the first one in Eq. (46) for the effective interaction which links only positive-energy plane waves clearly show this nonlinearity in the density. The similarity of the results from these two different effects suggests that Pauli effects from the nuclear medium may be an important element in unravelling the purely relativistic content of the NN t matrix for scattering from a bound nucleon. It is possible that in the separate treatments of both relativistic effects and medium effects, they each have been overestimated. A more coordinated theoretical approach is called for.

Since data will soon become available for proton scattering from ^{40}Ca at 650 MeV, we show the relativistic and nonrelativistic predictions at this energy in Fig. 3.

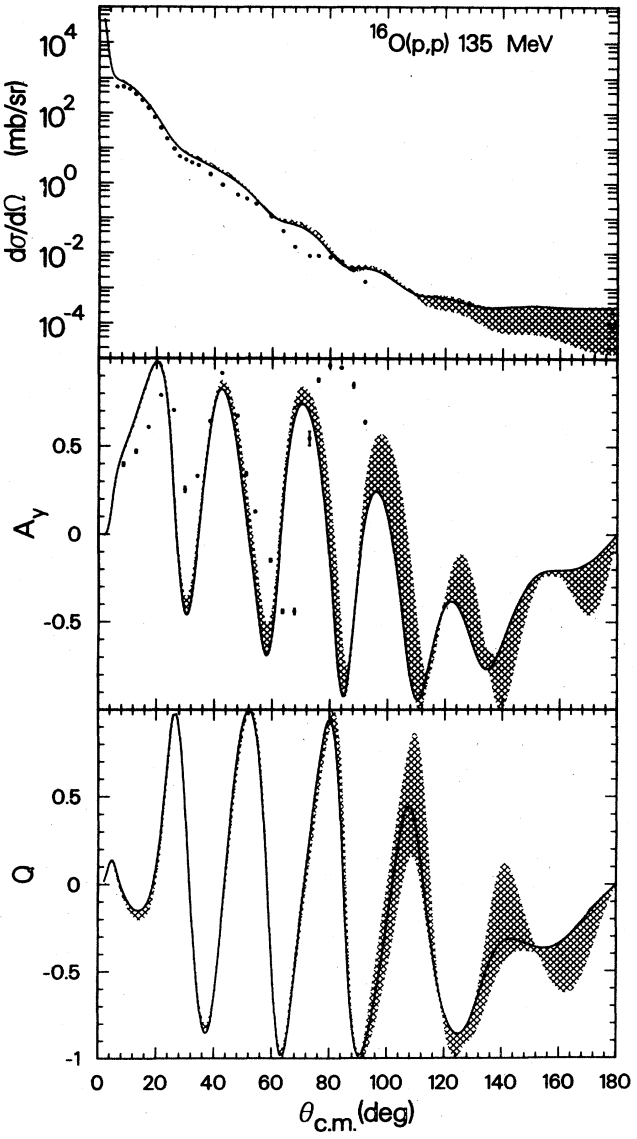

FIG. 10. Same as for Fig. 8, except for ^{16}O at 135 MeV and the data are from Ref. 19.

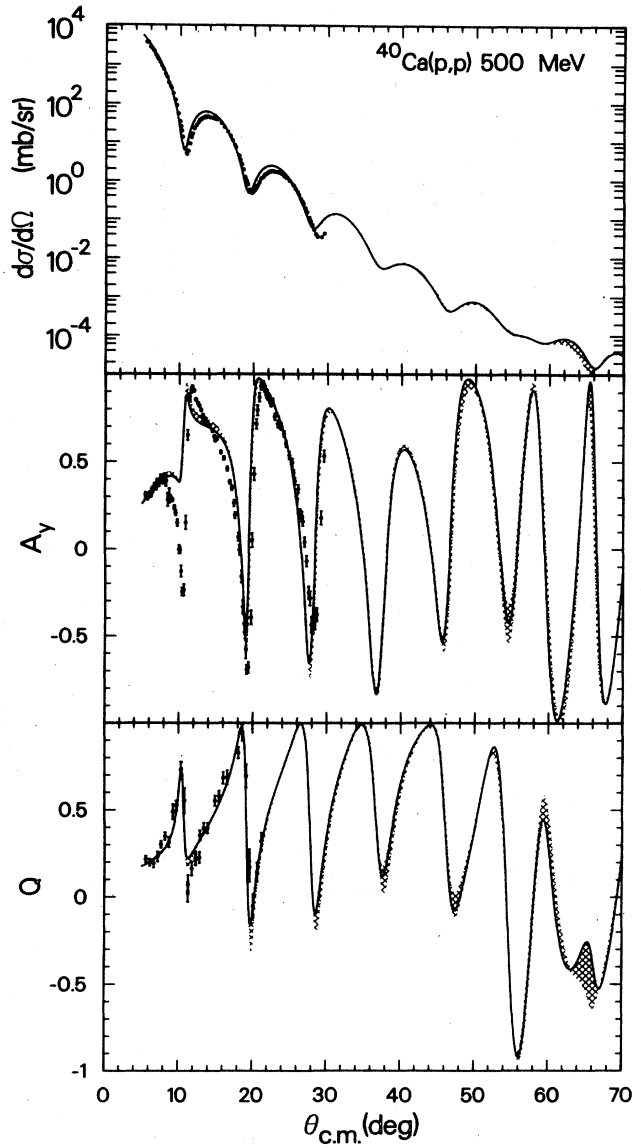

FIG. 11. Same as for Fig. 8, except that here an increased range of scattering angle is displayed.

The difference between the two predictions for the differential cross section is similar to that at 500 MeV. The nonrelativistic result again has sharper minima and is somewhat more compact than the relativistic curve. The results for A_y and Q again show the characteristic phase difference at the first diffraction minimum and the deepening of higher-order minima. These qualitative differences should be easily distinguished by the data when it becomes available.

Comparisons of the relativistic and nonrelativistic predictions of $d\sigma/d\Omega$ and A_y for ^{40}Ca at 300 MeV have been presented elsewhere[4] and will not be repeated here. In this case, except for the region of the first diffraction minimum, the nonrelativistic calculations provide a better description of the data.

The data for ^{40}Ca at 500 MeV is, in fact, so well described by the relativistic approach that the performance over a wider regime demands to be explored. We do not, of course, expect that a parameter-free approach will invariably yield precise predictions everywhere. What we do hope is that the relativistic approach has an extended regime of applicability when compared to the nonrelativistic approach. Deviations from the predictions can then be interpreted as arising from physical effects not included in the theoretical framework or from inadequate approximations adopted within calculation. Much of the thrust of the *numerical* part of the present paper is to explore the regime of applicability of the relativistic approach, to investigate the sensitivity of the calculations to the uncertainties in the input, and to investigate the validity of various approximations which serve to facilitate computation.

With the foregoing in mind, we turn now to the scattering of medium energy protons from ^{16}O. In a previous

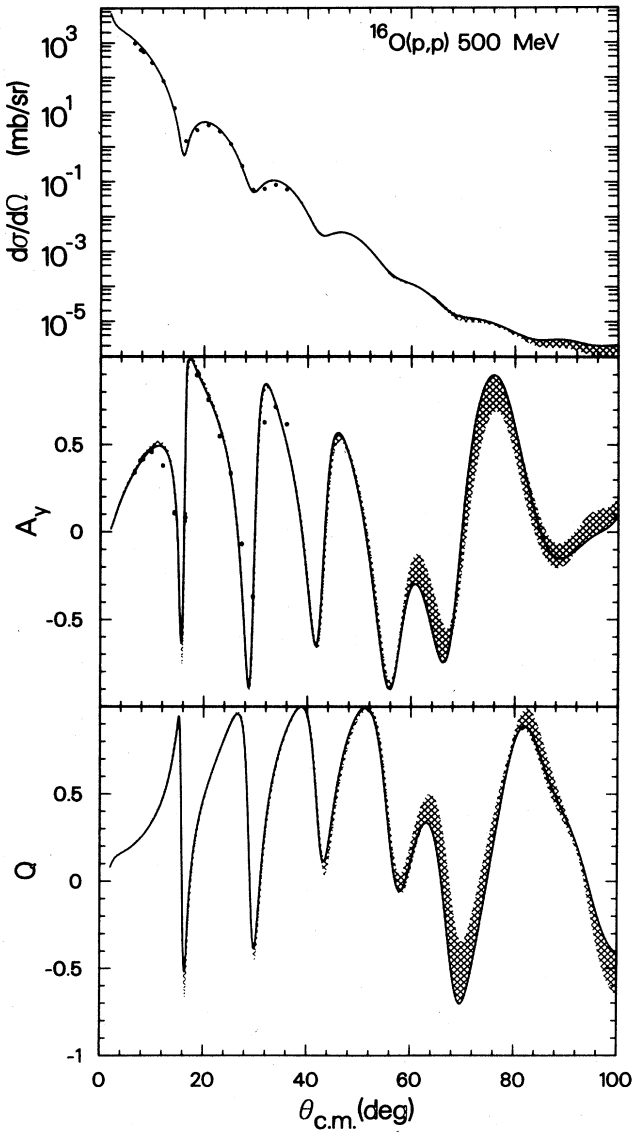

FIG. 12. Same as for Fig. 8, except for ^{16}O at 500 MeV and the data is from Ref. 26.

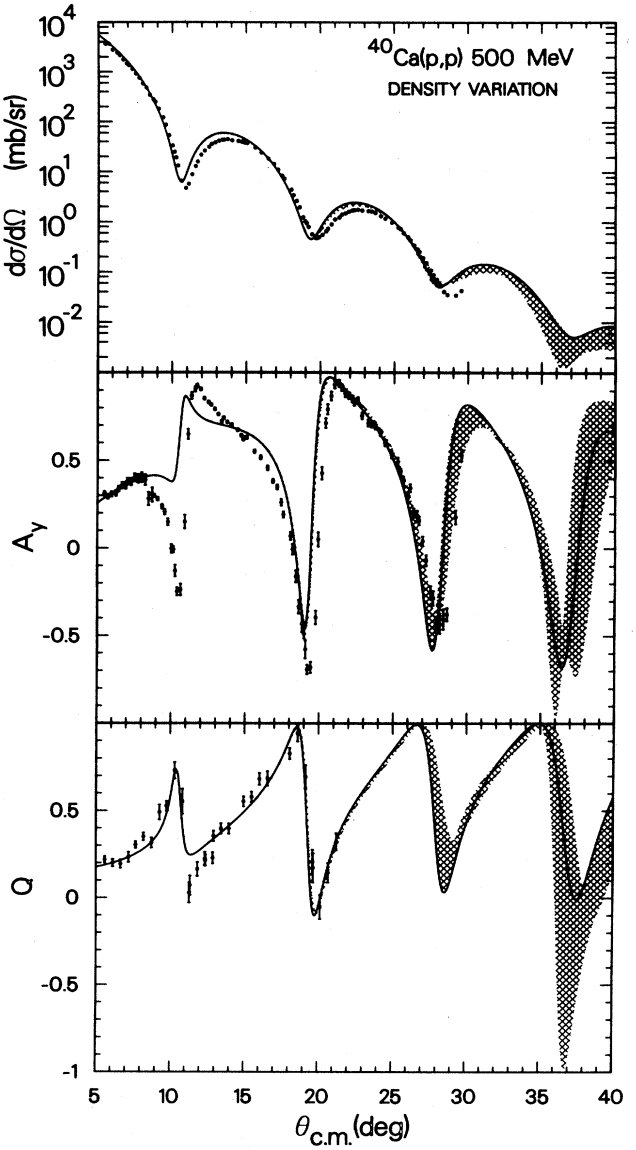

FIG. 13. Differential cross section, analyzing power, and spin rotation function for 500 MeV protons scattered from ^{40}Ca. The solid line corresponds to the same relativistic calculation displayed as a solid line in earlier figures. The cross-hatched areas represent the uncertainties due to incomplete knowledge of the nuclear density as described in the text. The data is from Ref. 24.

publication[4] the 500 MeV relativistic and nonrelativistic predictions for the cross section and analyzing power have been presented and compared with one another and with the data. In this case the nonrelativistic result provides a good description of the data which is further improved by the additional relativistic process described in this paper.

In Figs. 4 and 5 we present results for ^{16}O at 318 and 180 MeV. Extensive data will soon become available to test these predictions. The qualitative features of both calculations for 318 MeV are the same and the comparison is quite similar to the case of ^{40}Ca at 300 MeV. The sharp oscillatory structure for A_y and Q at forward angles is present in both the relativistic and nonrelativistic results in contrast to the case at several hundred MeV higher in energy. Preliminary data[20] agree well with the relativistic calculation for A_y and Q.

The energy of 180 MeV is rather low for the first-order free impulse approximation to the optical potential to be expected to perform well. The clear distinction between the relativistic and nonrelativistic results that was evident for a ^{40}Ca target at this energy (Fig. 2) is of the same character for the lighter target as seen from Fig. 5. Data for Q at 180 MeV on ^{16}O and ^{40}Ca at small angles should be highly instructive. Similar observations about the ^{16}O data at 135 MeV have been made in a previous publication.[4]

Overall, we observe that where the nonrelativistic predictions are far from the data, the differences between the

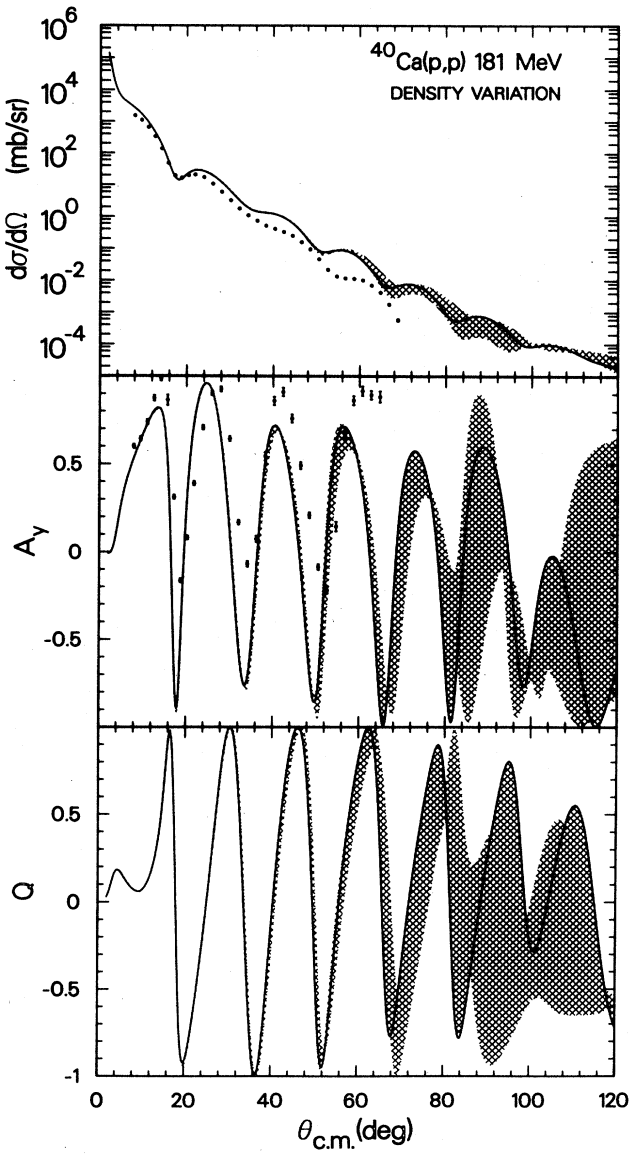

FIG. 14. Same as for Fig. 13, except that the energy is 181 MeV and the data are from Ref. 25.

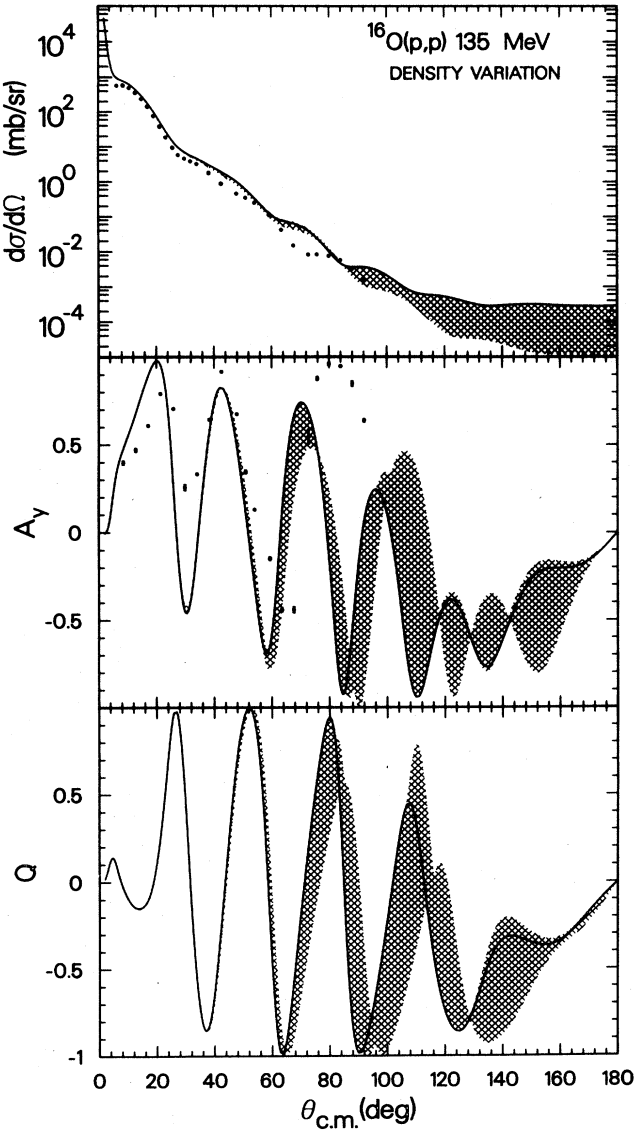

FIG. 15. Same as for Fig. 13, except for ^{16}O at 135 MeV and the data are from Ref. 19.

nonrelativistic and relativistic predictions are often dramatic, as for ^{40}Ca at 500 MeV, and the relativistic result is in far better accord with the data. Where the nonrelativistic predictions are in good qualitative agreement with the data, the relativistic addition turns out to be small, and in the appropriate direction to improve the description of the data. Thus the arguments in favor of the relativistic addition are cumulatively compelling, provided that we are able to rule out sensitivity to other effects not included in these first-order calculations, which might be large enough to change our conclusions. In the latter part of this section we present the results of tests designed to explore this question.

In Figs. 6 and 7 we compare relativistic and nonrelativistic calculations for ^{40}Ca and ^{16}O at 500 MeV for larger momentum transfers, out to about $7F^{-1}$. A number of uncertainties which are unimportant for small q can enter in a significant way at larger momentum transfer. As we will see later, the major source of ambiguity is the lack of constraint on the nuclear density. This is due to the limited range of electron scattering information. Figures 6 and 7 indicate that with a fixed representation of the nuclear density as a three-parameter Fermi shape, the relativistic and nonrelativistic calculations yield the same qualitative behavior for the larger momentum transfers shown. Of the number of small effects that can contribute significantly to these numerically difficult first-order calculations,[4] we have found that Coulomb-nuclear interference effects are quite important for A_y and Q at large momentum transfer.

In Fig. 7 it is noteworthy that the qualitative behavior of A_y and Q for the first diffraction minimum is given correctly for ^{16}O at 500 MeV by both the relativistic and nonrelativistic results. We must view the contrasting situ-

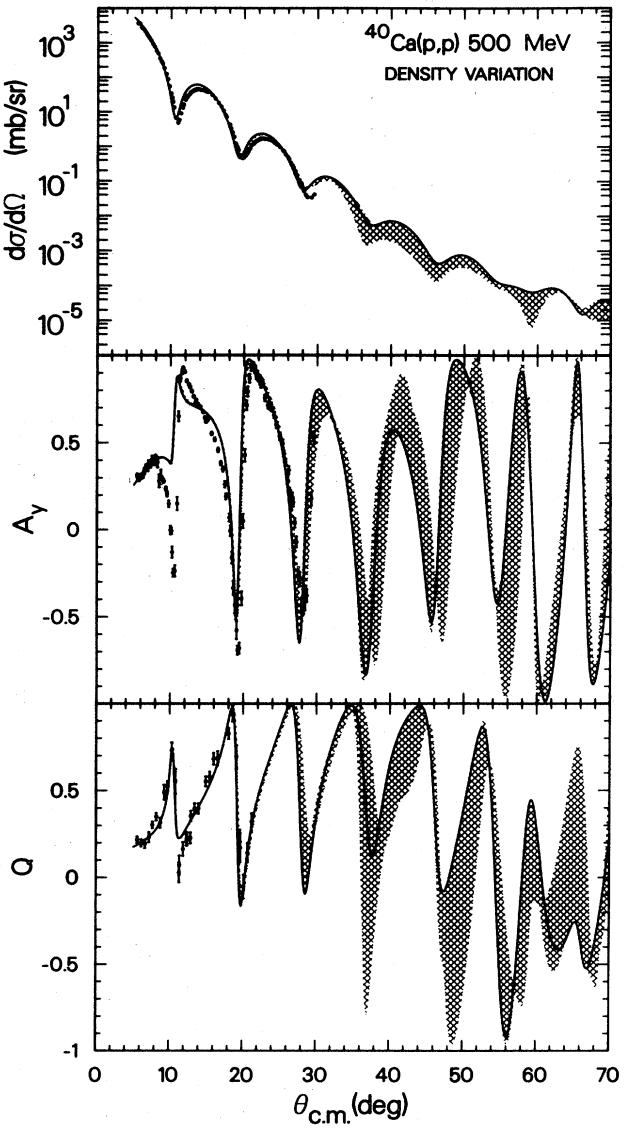

FIG. 16. Same as for Fig. 13, except that here an increased range of scattering angle is displayed.

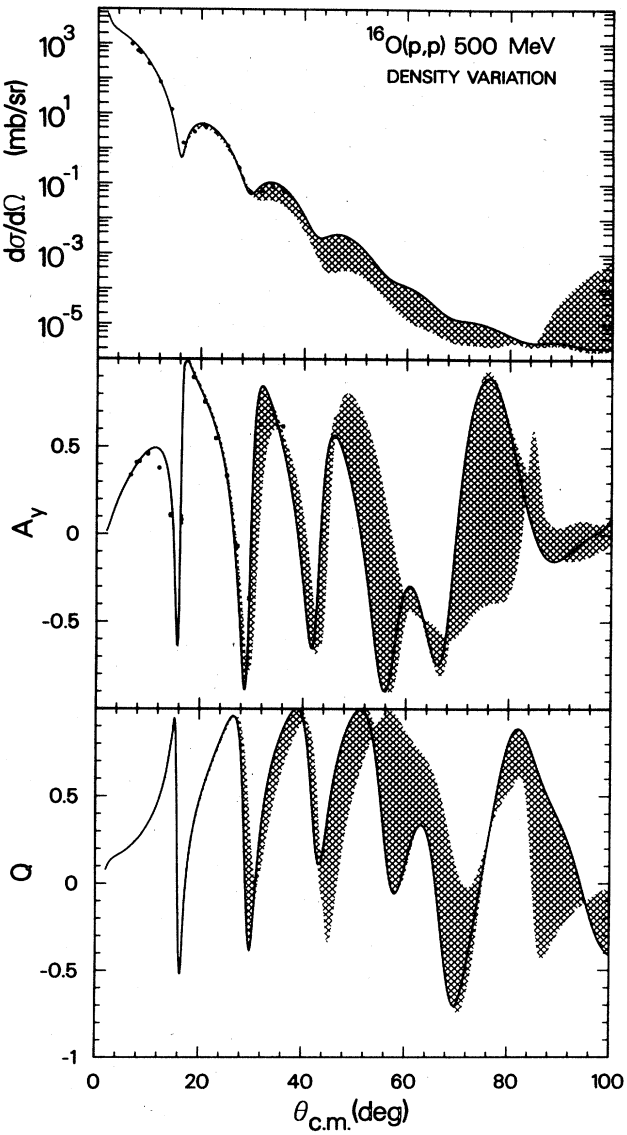

FIG. 17. Same as for Fig. 13, except for ^{16}O at 500 MeV and the data are from Ref. 26.

ation for ^{40}Ca at the same energy as evidencing a special sensitivity to the particular nuclear shape.

B. Off-shell and nonlocal effects

We now wish to explore the sensitivity of the relativistic calculations which we have presented to off-shell and nonlocal effects. By these effects we mean the dependence upon $\mathbf{K}=\frac{1}{2}(\mathbf{k}'+\mathbf{k})$ as well as upon q in Eqs. (37) and (38) for the components of $U^{++}(\mathbf{k}',\mathbf{k})$. Since the complete relativistic optical potential in this work is inferred from this nonrelativistic piece, off-shell and nonlocal dependence will be induced in the components U^{+-}, U^{-+}, and U^{--}. We assume this to be representative of the character of such effects that would be obtained from a more fundamental calculation of the relativistic components of the NN t matrix. In all instances we find that the sensitivity calculated in the relativistic case follows fairly closely the findings for the nonrelativistic case.[1] This sensitivity is displayed in Figs. 8–12.

We do not consider the standard local, on-shell factorization prescription $[t(q)\rho(q)]$ that has been almost invariably employed in representations of the first-order KMT optical potentials. From the studies presented in Ref. 1, we observe that, although this rather crude approximation to the first-order optical potential gives reasonable results for scattering angles below $\sim 30°$, the approximation becomes progressively worse beyond $\sim 30°$ and has no clear meaning beyond $\sim 60°$.

The solid curves in Figs. 8–12 result from the optimum factorization procedure in which the optical potential is nonlocal and includes particular off-shell extrapolations of the nucleon-nucleon t matrix. The calculations are identical to those shown as solid lines in Figs. 1–7.

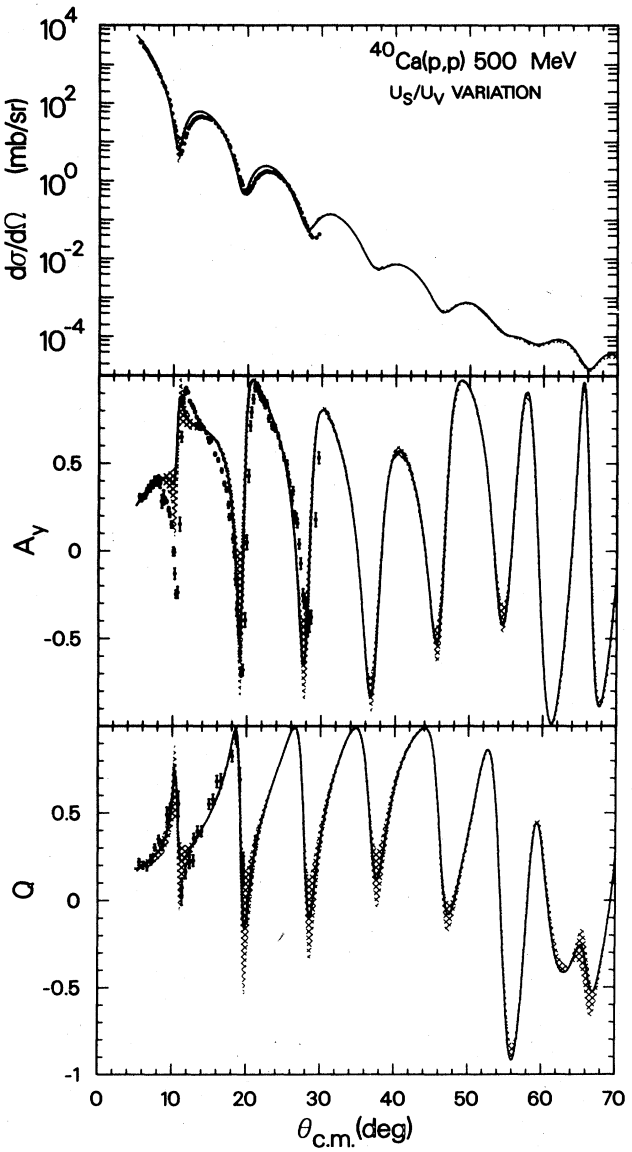

FIG. 18. Differential cross section, analyzing power, and spin rotation function for 500 MeV protons scattered from ^{40}Ca. The solid line corresponds to the same relativistic calculation displayed as a solid line in earlier figures. The cross-hatched areas represent the effect of ±1% variations in the Lorentz scalar and vector composition of the optical potential employed here. The data is from Ref. 24.

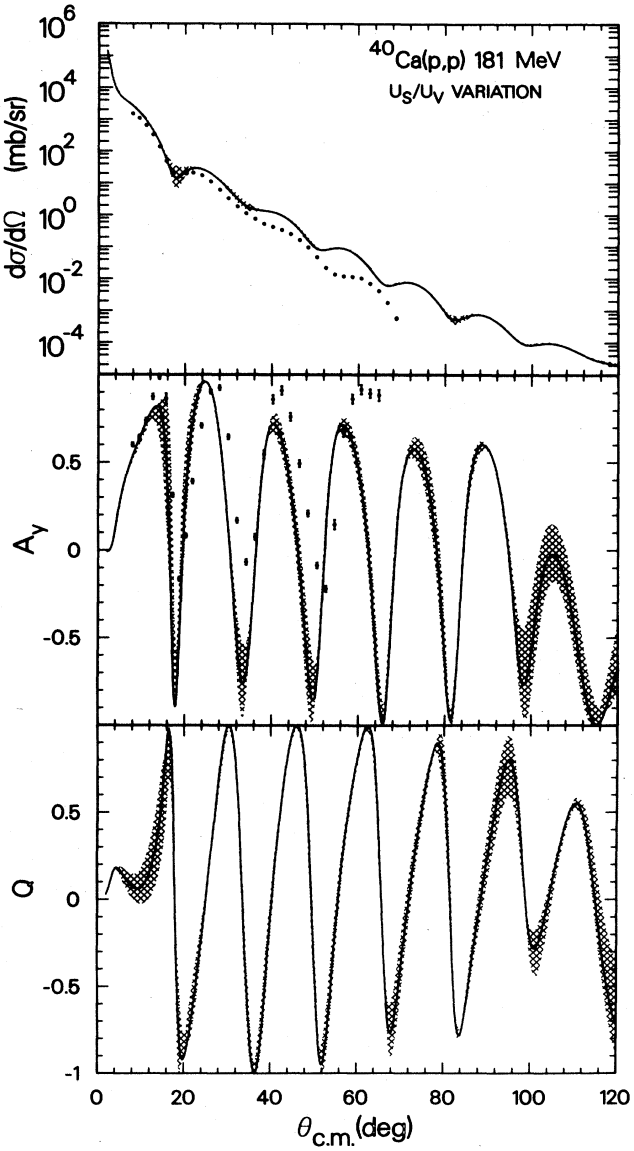

FIG. 19. Same as for Fig. 18, except that here the energy is 181 MeV and the data are from Ref. 25.

The energy of the nucleon-nucleon t matrix is fixed at the value corresponding to the nucleon-nucleon scattering at the beam energy. The shaded regions in Figs. 8—12 are intended as an estimate of the uncertainty introduced by the use of a factorization approximation instead of performing the full-folding integral in the calculation of the first-order optical potential. The variations away from the optimum factorization result introduced by the asymptotic momentum approximation for the nonlocality of the exchange terms, and also by the variation in the energy of the NN t matrix as prescribed using the invariant NN mass, have been used to define the shaded regions in Figs. 8—12. These may be viewed as yielding an indication of the typical size of off-shell and nonlocal effects. Further details and discussion of the estimation of these effects is given in detail in Ref. 1. Here these same calculations are performed in the relativistic case.

In Figs. 8—12 the estimated off-shell and nonlocal effects are displayed at the higher and lower ends of the 100—500 MeV range. In the region where data currently exist at 500 MeV, the uncertainty represented by the shaded band is rather small. This engenders further confidence in any conclusions we may draw from the comparison of relativistic first-order calculations and the 500 MeV ^{40}Ca data. We have seen similar insensitivity in the nonrelativistic calculations at this energy. Clearly for ^{40}Ca at 500 MeV, nonlocal—off-shell uncertainties can be considered to have a negligible effect on interpretation of

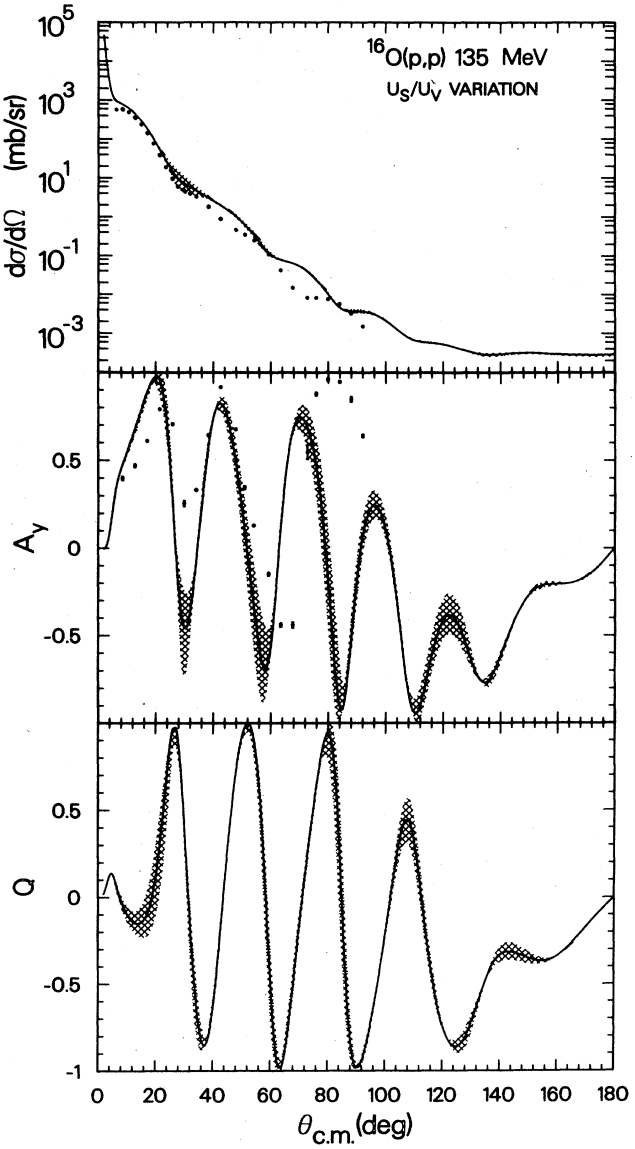

FIG. 20. Same as for Fig. 18, except for ^{16}O at 135 MeV and the data are from Ref. 19.

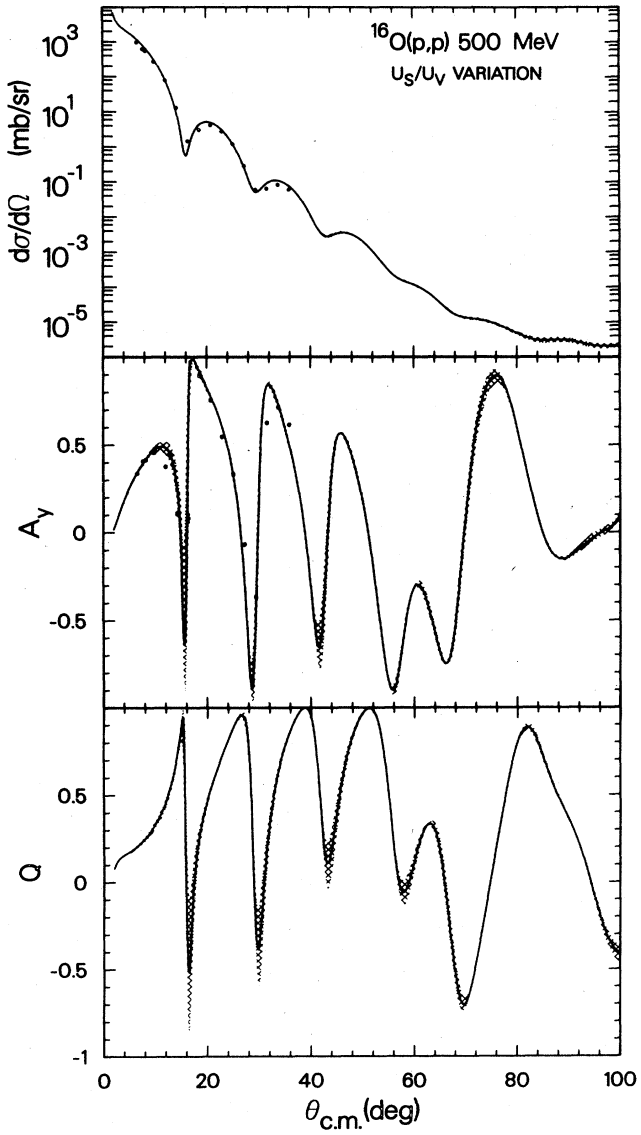

FIG. 21. Same as for Fig. 18, except for ^{16}O at 500 MeV and the data are from Ref. 26.

the results.

At a given energy, the influence of these effects increases with scattering angle and is more evident in A_y and Q than in the differential cross section. Also, these effects become more significant with decreasing energy as can be seen in Figs. 9 and 10. The task of unraveling the ambiguities in formulations of the relativistic impulse approximation at energies near and below 100 MeV must address the nonlocal and off-shell character of the NN t matrix and the related question of how this is to be accurately combined with the nuclear bound state information. Figures 11 and 12 confirm that even at large momentum transfer the high energy scattering observables are not likely to be significantly influenced by off-shell and nonlocal aspects of the relativistic optical potential.

C. Uncertainties in the nuclear densities

In Figs. 13—17 we show the results of relativistic calculations in which the nuclear densities are taken from different sources. The solid curve has the same meaning as in previous figures and corresponds to a nuclear density described as a three-parameter Fermi shape with the parameters taken from a compilation of electron scattering analysis.[18] The variations away from this solid curve, obtained from the use of two other sources of nuclear densities, are shown as a shaded band. The two alternative sources of nuclear density information are: (1) a shell model calculation[21] using Woods-Saxon single particle potentials with the various parameters constrained by energy level, transition rate, and electron scattering information;

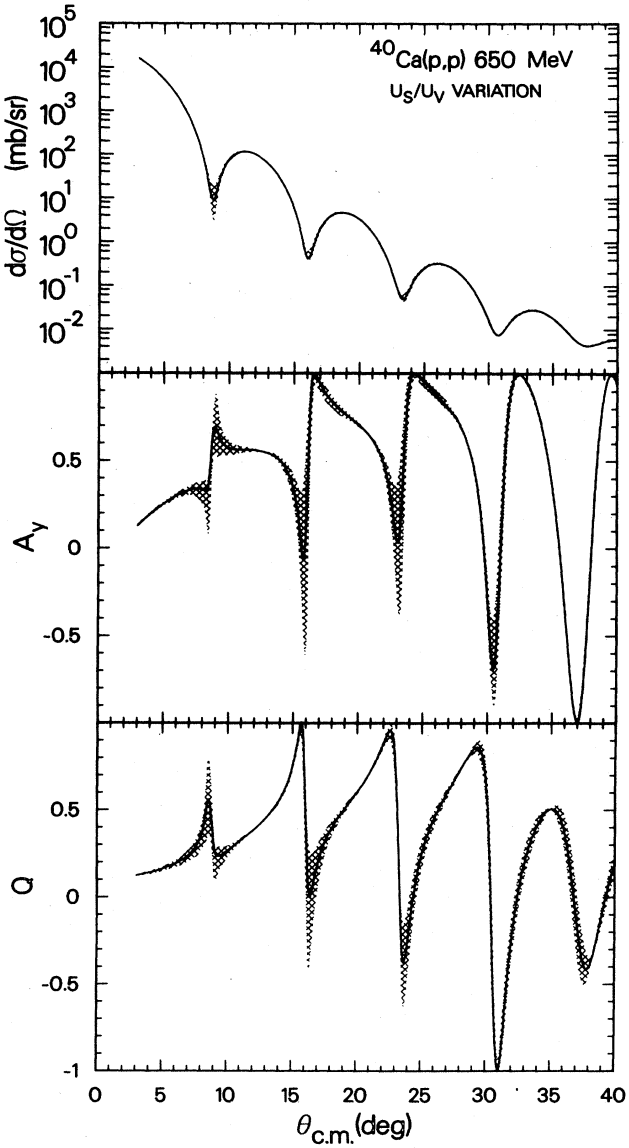

FIG. 22. Same as for Fig. 18, except at 650 MeV.

and (2) fits to electron scattering form factors in terms of a three-parameter Fermi shape supplemented by other functions to improve the description of the data at high momentum transfer.[22] In the shell model case, the point neutron and proton densities are not identical, while in the second case the point neutron density is taken to be identical to the point proton density.

As one would expect, Figs. 13–17 illustrate that these differing descriptions of the nuclear density have essentially no effect on the calculated scattering observables for forward angles throughout the energy range above ~100 MeV. However, the model dependence of the nuclear density introduces uncertainties in the scattering observables which increase significantly with increasing momentum transfer. In all cases these ambiguities are the largest of all those considered in this paper. In Fig. 13 the nuclear density sensitivity for protons scattered from ^{40}Ca at 500 MeV is displayed. In the angular region in which data exist this uncertainty may be seen to be completely negligible and only becomes appreciable beyond ~35°. Comparison with the analogous nonlocal–off-shell sensitivity for the same case, shown in Fig. 8, clearly establishes how much less important is the specific treatment of off-shell effects than is a more complete knowledge of the nuclear distribution. As the energy is lowered or a lighter target is considered, the nuclear density ambiguities impinge upon regions where data exist or could soon be measured without difficulty, as indicated in Figs. 14 and 15.

Figures 16 and 17 serve to indicate that lack of knowledge of the large momentum transfer components of the density is the principal question that would be addressed by any future measurements of scattering observables in an extended angular range. Questions of the appropriate relativistic departures from nonrelativistic first-order descriptions would seem to be of secondary importance, as are off-shell and nonlocal effects.

D. Specifically relativistic sensitivity

In Figs. 18–22 we examine the sensitivity of the relativistic results for the scattering observables to variation of the scalar and vector composition of the optical potential. One motivation for such a study comes from the fact that S and V are separately each large and of opposite sign. In the nonrelativistic sector, the spin-independent central part of the optical potential is described by the sum of S and V. Thus we might expect any uncertainty in S and/or V to be magnified in the determination of the central potential.

Another motivation for this study is that the scalar and vector components of the optical potential adopted in this work can only be viewed as effective components. The form of $U^{++}(\mathbf{k}',\mathbf{k})$, the nonrelativistic sector of the optical potential, can be reproduced by a structure for the operator U in Dirac spinor space which is more general than the structure $U=S+\gamma^0 V$ considered here. For example, a dependence upon gamma matrices γ and $\sigma^{\mu\nu}$ is to be expected in the general case. The general relativistic description will remain quite model dependent until components of the target states and the NN t matrix that have the corresponding transformation properties are under reliable theoretical control. In this light, an effective scalar and vector representation is model dependent and the results reported in the following give an indication of how this can be expected to affect calculated scattering observables.

In this study we have used only a single parameter to display this sensitivity. We have taken $S'(\alpha)=(1+\alpha)S$, and varied the parameter about $\alpha=0$. For ^{40}Ca 500 MeV the case $\alpha=0.01$ provides an essentially perfect fit to the data. With this in mind, we display in Figs. 18–22 the result for $\alpha=0.0$ as a solid line, and the shaded band is defined by the limits $\alpha=\pm 0.01$. This band of width 2% is seen to have a negligible effect on the differential cross sections but a significant effect on the minima and maxima of the spin-dependent observables A_y and Q. In particular, we note that for ^{40}Ca at the energies of 500 and

650 MeV, the qualitative behavior in the region of the first diffraction minimum is subject to a large variation. For the same target at the lower energy of 181 MeV, and also for an ^{16}O target at the energy of 500 MeV, the qualitative behavior of A_y and Q in the region of the first diffraction minimum is stable to this uncertainty. The contrast in the behavior at the first diffraction minimum for 500 MeV scattering from ^{16}O and ^{40}Ca must be viewed as an effect based primarily on the difference between the momentum-space structure of the density profile of the target.

By comparing Figs. 18—22 with earlier figures, we can see that small ambiguities in the effective scalar and vector composition are much more significant at small scattering angles than is the lack of precise knowledge of either the off-shell and nonlocal structure of the NN t matrix or the nuclear density profile.

V. SUMMARY

In this paper we have investigated a variety of the relativistic aspects that arise in a Dirac equation description of proton-nucleus elastic scattering with an ansatz for a first-order microscopic optical potential. We have discussed the utility of a formulation of this problem in terms of a momentum-space integral equation for the transition amplitude. In this approach, the optical potential can be expressed as a 2×2 matrix with elements U^{++}, U^{+-}, U^{-+}, and U^{--}. Each of these quantities depend upon $\mathbf{k}'$, $\mathbf{k}$, and $\boldsymbol{\sigma}$, the Pauli operator for the spin of the projectile nucleon. They are the projections of the relativistic operator U for the nucleon-nucleus optical potential onto the positive and negative energy states of a free Dirac particle. The coupled integral equations given in the text for the components T^{++} and T^{-+} are equivalent to the Dirac wave equation in which the interaction operator is U. The microscopic content of the relativistic nucleon-nucleus operator U that corresponds to a first-order mechanism in a multiple scattering framework is not settled at present. In large measure, this is due to the absence of a multiple scattering *expansion* for a problem which is inherently a field-theoretical one.

We have argued that if negative energy plane wave expansion components of the target states are ignored, then the component U^{++} should reduce to the nonrelativistic optical potential when a first-order scattering mechanism is adopted. The subsequent microscopic considerations of this paper are built around this constraint. We adopt a simple ansatz for the relativistic operator U so that the resulting U^{++} reproduces the nonrelativistic first-order optical potential that we have calculated and applied in recent work.[1] This U^{++} contains microscopically based nonlocalities and off-shell effects from the NN t matrix. The simple relativistic extension ansatz is that U^{++} be viewed as the positive-energy Dirac spinor matrix element of the operator $U=S+\gamma^0 V$. The deduced scalar and vector components are then used to construct the purely relativistic quantities U^{+-}, U^{-+}, and U^{--}. Off-shell effects and nonlocalities are included in these quantities through their forced relationship to U^{++}. This extension ansatz is not unique. It can be viewed as the nucleon-nucleus counterpart of the related ansatz applied at the nucleon-nucleon level in initial works[2] on the construction of a first-order optical potential for a Dirac equation. The topic of the frame transformation for the NN scattering amplitude is treated within the construction of U^{++} and is divorced from the topic of the extension from positive to negative energy basis states.

Part of the motivation for the studies undertaken in this paper is to see whether the essential features that distinguish the numerical results of relativistic first-order prescriptions from those of the nonrelativistic first-order calculations are reproduced by the simpler extension ansatz. In large measure, we find this to be so. The single notable exception is the very forward angle behavior of the spin-dependent observables in elastic proton scattering from ^{40}Ca at 500 MeV. There we find the qualitative behavior of the calculations to be extremely sensitive to small variations in the assumed vector and scalar composition of the relativistic nucleon-nucleus operator U. At the same energy, with the target nucleus taken to be ^{16}O and all other aspects of the calculation taken to be identical, there is no comparable sensitivity in the qualitative structure of the spin-dependent observables. The situation for a ^{40}Ca target at this energy must be considered an effect driven in large part by the particular shape of this nucleus. The model dependence of relativistic representations of the NN t matrix and the underlying framework for a multiple scattering representation of a field-theoretical system would have to be under much tighter control than at present to confidently explain the behavior in this case. An important step in this direction would be provided by an independent calculation of the positive and negative energy plane-wave matrix elements of the NN scattering operator.

We have discussed the nature of the extra processes that enter when the projectile is treated as a Dirac particle rather than as a Schrödinger-Pauli particle. The new processes enter because of the relativistic enlargement of the Hilbert space to include the negative-energy states of a free particle. The use of NN scattering amplitudes that fit NN data implicitly include negative energy plane-wave intermediate states in the two-body operators. In the many-body situation such intermediate states necessarily enter between the projectile's scattering from two different target nucleons. The nucleus can remain in the ground state between such scatterings. However, this is not part of the elastic channel. The lowest-order relativistic correction in the *effective* elastic channel optical potential is therefore a three-body (projectile plus two nucleons of the target) term. No pair correlations of the target are needed to feed such a term in contrast to the requirement for a three-body term in the nonrelativistic multiple scattering expansion. A definition of a first-order multiple scattering mechanism for an optical potential which is broad enough to cover both circumstances would be the absence of mechanisms requiring pair correlations in the target.

The comparison of relativistic and nonrelativistic calculations of scattering observables over the energy range 100—500 MeV indicates that the relativistic effects are very important for spin-dependent observables at all ener-

gies investigated. Where data exist, the agreement is improved compared to the nonrelativistic calculations of these observables. The agreement with cross section data is improved at the higher energies but not at the lower energies. This may reflect the importance of Pauli effects, higher-order multiple scattering terms, and inadequate knowledge of relativistic features of NN t matrices. The most interesting and obvious relativistic effects occur at low momentum transfer. This offers the opportunity of possible further refinement in our knowledge of such effects, unencumbered by serious contributions from correlative effects if the energy is not too low.

The nonlocality and off-shell effects present in the optical potential are investigated in a way which gives an estimate of the ambiguity due to use of a factorization prescription instead of carrying out the integral for the nuclear ground state matrix element of an intrinsically nonlocal NN scattering operator. As in the nonrelativistic case, such ambiguities are quite negligible at energies above about 300 MeV for moderate momentum transfer. As the energy is lowered, such ambiguities become more serious and occur at smaller momentum transfer where data exist or can reasonably be measured. The characteristic influence of the relativistic effects on the spin-dependent observables still survives after consideration of these ambiguities.

At moderate and large momentum transfer, the most serious uncertainty comes from the lack of detailed knowledge of the nuclear shape. By using several different sources for the nuclear density profile, we confirm that the low q relativistic effects remain identifiable, while the task of identifying such affects at moderate q is masked by the uncertain knowledge of the density.

Variations of $\pm 1\%$ in the vector-scalar composition of the optical potential are used to display estimations of the effect of typical ambiguities in arriving at the microscopic content of the operator that should go into a Dirac equation for elastic scattering. There are negligible effects on the differential cross sections but quite significant effects on the sharpness of minima and maxima of the spin-dependent observables. The most serious effects are at low q, where this type of model dependence is much stronger than all other effects we have investigated. The qualitative structure of the angular distributions for A_y and Q is maintained in all cases except for the sharp oscillation at low q for scattering from ^{40}Ca at 500 and 650 MeV.

Given the ill-defined nature of the theoretical framework at present, relativistic treatments of elastic nucleon-nucleus scattering produce results which, overall, are in better accord with data than the corresponding nonrelativistic treatment. Further refinement of the theoretical framework, which takes a relativistic viewpoint close to field theory from the beginning, is called for. In this regard, it should be emphasized that neither the approach adopted in this work nor the approach of Refs. 2 is very far removed from the phenomenological investigations of Ref. 15. The results of Refs. 2 and the relativistic-nonrelativistic comparisons of this work depend crucially upon an ansatz. In both cases, the ansatz yields vector-scalar dominance of the optical potential and, almost as a consequence, the characteristic advantages of Ref. 15. Nevertheless, the link between the phenomenology of Ref. 15 and the microscopic nonrelativistic optical potential obtained here and in Refs. 2 is both physically and intuitively exciting. Confirmation of the qualitative physical correctness of the results obtained on the basis of current approaches, however, must await comprehensive studies with microscopically based sources of the full Dirac t matrix and, more importantly, a sound theoretical justification.

ACKNOWLEDGMENTS

Three of us (A.P., P.C.T., R.M.T.) wish to acknowledge the support of the Los Alamos National Laboratory especially during a number of visits throughout the course of this work. The Los Alamos National Laboratory is operated by the University of California for the U.S. Department of Energy under Contract No. W-7405-ENG-36. Partial support was provided by the U.S. Department of Energy under Grant No. DE-AS05-83-ER05126 and by the National Science Foundation under Grants No. PHY83-05745 and No. PHY81-21956.

APPENDIX

Our ansatz for obtaining the Dirac optical potential from knowledge of the first order nonrelativistic optical potential, namely Eqs. (35)—(40) and the related discussion in the text, implies a specific treatment of the Lorentz transformation properties of the NN t matrix and of relativistic aspects of the intrinsic structure of the nuclear target. Here we set out and discuss these implications in order to allow comparison with other approaches[2] that begin with an ansatz for obtaining Lorentz invariant two-body amplitudes before the nucleon-nucleus interaction is constructed.

The purposes of the present discussion can be met by consideration of the simplified case in which the target nucleus is described in a single particle model and the mass of the target is taken to the large. The first order KMT nonrelativistic optical potential[10] can then be expressed in the form[1]

$$U_{\rm NR}(\mathbf{k}',\mathbf{k})=\frac{A-1}{A}\sum_i U_i(\mathbf{k}',\mathbf{k}) , \tag{A1}$$

where

$$U_i(\mathbf{k}',\mathbf{k})=\int d^3P\langle\phi_i\,|\,\mathbf{P}-\tfrac{1}{2}\mathbf{q}\rangle\langle\mathbf{k}',\mathbf{P}-\tfrac{1}{2}\mathbf{q}\,|\,t\,|\,\mathbf{P}+\tfrac{1}{2}\mathbf{q},\mathbf{k}\rangle\langle\mathbf{P}+\tfrac{1}{2}\mathbf{q}\,|\,\phi_i\rangle . \tag{A2}$$

Here the frame of reference is the frame of zero total momentum of the projectile plus nucleus system. The state $\langle \mathbf{p} \mid \phi_i \rangle$ is a nonrelativistic (Schrödinger) single particle state for the ith bound nucleon of the target, and $|\langle \mathbf{p} \mid \phi_i \rangle|^2$ is the probability density for that particle to have momentum p. The two-body t matrix in Eq. (A2) is an operator in the (Pauli) spin space of both particles, and $\mid \phi_i \rangle$ includes a (two-component) Pauli spinor. The notation of Eq. (A2) is meant to imply a scalar product in the spin space of the struck nucleon, so that the resulting $U_i(\mathbf{k}',\mathbf{k})$ is an operator in the (Pauli) spin space of just the projectile. Let $\mathbf{p}=\mathbf{P}+\frac{1}{2}\mathbf{q}$ and $\mathbf{p}'=\mathbf{P}-\frac{1}{2}\mathbf{q}$ be, respectively, the initial and final momenta of the struck nucleon that enter into Eq. (A2). We introduce a change of basis for the t-matrix element by writing

$$\langle \mathbf{k}',\mathbf{p}' \mid t \mid \mathbf{p},\mathbf{k} \rangle = \langle \overline{\mathbf{k}',+} \mid \langle \overline{\mathbf{p}',+} \mid t_D \mid \mathbf{p},+ \rangle \mid \mathbf{k},+ \rangle \ , \tag{A3}$$

where the basis states on the right-hand side of this equation are the positive-energy plane-wave Dirac spinors (each with four components) introduced in the text [see Eq. (18)]. The quantity t_D is an appropriate Lorentz invariant operator in the Dirac spinor space of both particles whose content is constrained only by the requirement that the right-hand side of Eq. (A3) reproduce the given left-hand side. This requirement does not determine the *operator* t_D uniquely, even if consideration is restricted to only on-shell values of the matrix elements in Eq. (A3). The ambiguities are of no consequence if attention is restricted to only positive energy Dirac plane wave states of the colliding pair of particles, as in the case under discussion at this stage.

The t-matrix elements in Eq. (A3) are defined in the frame of zero total momentum of the projectile-nucleus system and must be transformed to the frame of zero total momentum of the projectile-nucleon system in order to make use of available information for the t-matrix obtained in the latter frame. We introduce the state

$$\mid \mathbf{k},+ \rangle = \left[\frac{E(k)}{m} \right]^{1/2} \mid \mathbf{k},+ \rangle \tag{A4}$$

which has the normalization [cf. Eq. (7)]

$$(\overline{\mathbf{k}',+} \mid \mathbf{k},+) = \delta(\mathbf{k}'-\mathbf{k}) \ . \tag{A5}$$

Then, Eq. (A3) can be written as

$$\langle \mathbf{k}',\mathbf{p}' \mid t \mid \mathbf{p},\mathbf{k} \rangle = \left[\frac{m}{E(k')} \right]^{1/2} \left[\frac{m}{E(p')} \right]^{1/2} \times M(\mathbf{k}',\mathbf{p}';\mathbf{k},\mathbf{p}) \left[\frac{m}{E(k)} \right]^{1/2} \left[\frac{m}{E(p)} \right]^{1/2} , \tag{A6}$$

where

$$M(\mathbf{k}',\mathbf{p}';\mathbf{k},\mathbf{p}) = (\overline{\mathbf{k}',+} \mid \langle \overline{\mathbf{p}',+} \mid t_D \mid \mathbf{p},+ \rangle \mid \mathbf{k},+) \ . \tag{A7}$$

Let us consider for the moment that the required matrix element $\langle \mathbf{k}',\mathbf{p}' \mid t \mid \mathbf{p},\mathbf{k} \rangle$ describes a physically realizable two-body collision (one in which total four-momentum is conserved). Then there is a *single* Lorentz transformation which maps both the initial momentum pair $(\mathbf{p},\mathbf{k})$ and the final momentum pair $(\mathbf{p}',\mathbf{k}')$ into the corresponding values as seen from the frame of zero total two-body momentum.[23] Let the momenta in this two-body "center of mass" frame be $(-\not{k},\not{k})$ and $(-\not{k}',\not{k}')$ for the initial and final states, respectively. From the normalization condition [Eq. (A5)] of the spinors employed in Eq. (A7), the (on-shell) amplitude M is an invariant, that is

$$M(\not{k}',-\not{k}';\not{k},-\not{k}) = M(\mathbf{k}',\mathbf{p}';\mathbf{k},\mathbf{p}) \ . \tag{A8}$$

The t-matrix element in the two-body center of mass frame is given by

$$t(\not{k}',\not{k}) = \left[\frac{m}{E(\not{k}')} \right]^{1/2} \left[\frac{m}{E(\not{k}')} \right]^{1/2} M(\not{k}',-\not{k}';\not{k},-\not{k}) \times \left[\frac{m}{E(\not{k})} \right]^{1/2} \left[\frac{m}{E(\not{k})} \right]^{1/2} . \tag{A9}$$

With the left-hand side of Eq. (A9) determined from a two-body model, the t matrix required for the optical potential calculation (in the frame of zero total projectile-nucleus momentum) is obtained from Eqs. (A6), (A8), and (A9) in the form

$$\langle \mathbf{k}',\mathbf{p}' \mid t \mid \mathbf{p},\mathbf{k} \rangle = \eta(\mathbf{k}',\mathbf{p}';\mathbf{p},\mathbf{k}) t(\not{k}',\not{k}) \ , \tag{A10}$$

where the Moller factor for the change of frame is

$$\eta(\mathbf{k}',\mathbf{p}';\mathbf{p},\mathbf{k}) = \left[\frac{E(\not{k}')E(\not{k}')E(\not{k})E(\not{k})}{E(k')E(p')E(k)E(p)} \right]^{1/2} . \tag{A11}$$

The contribution of the ith nucleon of the target to the nonrelativistic first-order optical potential, from Eq. (A2), can now be written as

$$U_i(\mathbf{k}',\mathbf{k}) = \int d^3P \, \eta(\mathbf{P},\mathbf{k}',\mathbf{k}) \langle \phi_i \mid \mathbf{P}-\tfrac{1}{2}\mathbf{q} \rangle t(\not{k}',\not{k}) \langle \mathbf{P}+\tfrac{1}{2}\mathbf{q} \mid \phi_i \rangle \ , \tag{A12}$$

where $\not{k}'$ and $\not{k}$ depend upon $\mathbf{P}$ and where we have used the fact that η depends on only three independent momenta.

The method of optimum factorization that we employ for the approximation of the integral in Eq. (A12) consists of making a Taylor's series expansion of ηt in the variable $\mathbf{P}$ about a fixed value $\mathbf{P}_0$ chosen such that the contribution of the first derivative term is minimized. This point is $\mathbf{P}_0=0$ and the contribution of the first derivative term is zero there. Further details can be found in Ref. 1. Thus Eq. (A12) becomes

$$U_i(\mathbf{k}',\mathbf{k}) \approx \eta(\mathbf{P}=0,\mathbf{k}',\mathbf{k}) t(\not{k}_0',\not{k}_0) \rho_i(q) \ , \tag{A13}$$

where $\mathcal{K}'_0$ and $\mathcal{K}_0$ are evaluated at $\mathbf{P}=0$, but each still depends on $\mathbf{k}'$ and $\mathbf{k}$. The above-mentioned procedure for implementing the change of frame for the two-body t matrix is satisfactory for an on-shell two-body collision. However, only when the optical potential $U_i(\mathbf{k}',\mathbf{k})$ is on-shell ($k'=k$) does the two-body t matrix become on-shell ($\mathcal{K}'_0=\mathcal{K}_0$) in the optimally factorized form of Eq. (A13). In the general case one could attempt to deal with the Dirac operator t_D rather than the amplitude M. However this procedure requires prior knowledge of the t matrix on the complete Dirac space spanned by both positive and negative energy plane wave states, that is, a more complete relativistic model of projectile-nucleon scattering. Such considerations lie outside the scope of this paper.

Let us now consider the implications that the above treatment has for relativistic aspects of the initial and final bound nucleon states. We suppose, for the sake of this discussion, that the NN operator t_D in the Dirac spinor space has been suitably identified. We also suppose that the target nucleus is described by a single-particle model in which the states are Dirac states. Let $\langle \mathbf{r} \mid \psi \rangle$ be the Dirac single particle state corresponding to total angular momentum projection m within a filled subshell with quantum numbers j and l. This four-component spinor can be written

$$\langle \mathbf{r} \mid \psi \rangle = \begin{bmatrix} F_j(r)\mathcal{Y}^m_{jl}(\hat{r}) \\ -iG_j(r)\mathcal{Y}^m_{\bar{j}l}(\hat{r}) \end{bmatrix}, \tag{A14}$$

where the (scalar) functions $F_j(r)$ and $G_j(r)$ are the standard upper and lower components, $\bar{l}=2j-l$ and the $\mathcal{Y}^m_{jl}$ are the (Pauli) spinor-spherical harmonics defined in the text. We choose the normalization condition

$$\langle \psi \mid \psi \rangle \equiv \langle \bar{\psi} \mid \gamma^0 \mid \psi \rangle = \int d^3r\, \psi^\dagger(\mathbf{r})\psi(\mathbf{r}) = 1 . \tag{A15}$$

A simple relativistic extension of the component $U_i(\mathbf{k}',\mathbf{k})$ of the nonrelativistic optical potential which connects positive energy Dirac plane wave states of the projectile, would be written as

$$U_i^{++}(\mathbf{k}',\mathbf{k}) = \langle \overline{k',+} \mid \overline{\langle \psi} \mid t_D \mid \psi \rangle \mid \mathbf{k},+ \rangle . \tag{A16}$$

The substitution of negative energy plane-wave spinors for one or both of the projectile states would complete the description of the required Dirac optical potential.

To relate the U_i^{++} of Eq. (A16) to the nonrelativistic situation it is convenient to expand the state $\mid \psi \rangle$ in terms of Dirac momentum eigenstates. We thus write

$$\langle \mathbf{r} \mid \psi \rangle = \int d^3p [\langle \mathbf{r} \mid \mathbf{p},+ \rangle \psi_+(\mathbf{p}) + \langle \mathbf{r} \mid \mathbf{p},- \rangle \psi_-(\mathbf{p})] , \tag{A17}$$

where the components are operators in Pauli spin space and are given by

$$\psi_\pm(\mathbf{p}) = \langle \mathbf{p},+ \mid \psi \rangle . \tag{A18}$$

Substitution of Eq. (A17) into Eq. (A16) yields

$$U_i^{++}(\mathbf{k}',\mathbf{k}) = \int d^3P\, \psi^\dagger_+(\mathbf{P}-\tfrac{1}{2}\mathbf{q}) \langle \overline{\mathbf{k}',+} \mid \overline{\langle (\mathbf{P}-\tfrac{1}{2}\mathbf{q}),+} \mid t_D \mid (\mathbf{P}+\tfrac{1}{2}\mathbf{q}),+ \rangle \mid \mathbf{k},+ \rangle \psi_+(\mathbf{P}+\tfrac{1}{2}\mathbf{q}) + \Delta U_i^{++}(\mathbf{k}',\mathbf{k}) , \tag{A19}$$

where $\Delta U_i^{++}(\mathbf{k}',\mathbf{k})$ represents the three terms which involve the negative-energy plane-wave components of the initial and/or the final bound nucleon states. These components are very small compared to the $\psi_+(\mathbf{p})$. If they were to be neglected, then $\Delta U_i^{++}=0$. The first term of Eq. (A19) is exactly of the same form as the nonrelativistic optical potential of Eq. (A2), with the component ψ_+ playing the same role as the state ϕ. The physical content of ψ_+ and ϕ is, of course, very similar but not, in general, identical when separate dynamical models are employed for each. However, the neglect of negative-energy Dirac plane-wave components of nuclear bound states does restrict the physical picture involved in U_i^{++} to precisely that involved in the nonrelativistic counterpart U_i.

With ψ_- set to zero, consider now the optimum factorization procedure applied to the first term of U_i^{++} in Eq. (A19). If the full t-matrix element (i.e., including the Dirac spinor basis states) is evaluated at $\mathbf{P}=0$ and removed from the integral, the result is

$$U_i^{++}(\mathbf{k}',\mathbf{k}) \approx \langle \overline{\mathbf{k}',+} \mid \overline{\langle -\tfrac{1}{2}\mathbf{q},+} \mid t_D \mid \tfrac{1}{2}\mathbf{q},+ \rangle \mid \mathbf{k},+ \rangle \times \rho_{++}(q) , \tag{A20}$$

where the density $\rho_{++}(q)$, defined by

$$\rho_{++}(q) = \int d^3p\, \psi^\dagger_+(\mathbf{p}-\tfrac{1}{2}\mathbf{q})\psi_+(\mathbf{p}+\tfrac{1}{2}\mathbf{q}) , \tag{A21}$$

is a measure of the probability of imparting momentum $-\mathbf{q}$ to a target nucleon which initially and finally is in a positive-energy plane-wave component of the bound state. When ψ_- is not neglected the three terms that constitute $\Delta U_i^{++}(\mathbf{k}',\mathbf{k})$ have a structure similar to Eqs. (A20) and (A21) with the initial and/or the final bound nucleon labels ($+$) replaced by ($-$). In an obvious schematic notation the full U_i^{++} could be written

$$U_i^{++} = t^{++}_{++}\rho_{++} + t^{++}_{+-}\rho_{+-} + t^{++}_{-+}\rho_{-+} + t^{++}_{--}\rho_{--} . \tag{A22}$$

The last three terms of Eq. (A22) correspond to the three "Z graphs" described by Celenza and Shakin[3] for the diagrammatic expansion of the "one-body" density matrix associated with a relativistic "$t\rho$" approximation. Since the appearance of negative energy plane-wave basis states is a natural and convenient signature of processes coming from the relativistic enlargement of the Hilbert space, we feel that an organization of theoretical and calculational investigations along the lines suggested by Eq. (A22) has significant advantages and should be pursued. In the absence of firmly based information at this stage on the negative-energy plane-wave projections of t matrices and density matrices, we have taken only the first term of Eq. (A22) in this work and employed the simple ansatz as discussed in the text, for estimating the U_i^{+-}, U_i^{-+}, and U_i^{--} from U_i^{++}. That is, our approach can be described as taking the full Dirac optical potential to be given by

the four quantities

$$U_i^{\pm\pm}(\mathbf{k}',\mathbf{k}) \approx \langle \overline{\mathbf{k}',\pm} \mid \langle \overline{-\tfrac{1}{2}\mathbf{q},+} \mid t_D \mid \tfrac{1}{2}\mathbf{q},+ \rangle \times \mid \mathbf{k},\pm \rangle \rho_{++}(q) , \tag{A23}$$

where the "effective" (two-body) t_D is assumed to retain, after a spin average in the target space, a Dirac scalar and vector (fourth component only) parts ($t_D = t_S + \gamma_2^0 \gamma_1^0 t_V$) determined from equating U_i^{++} to the nonrelativistic counterpart U_i.

The last point we wish to make in this Appendix is that, from this point of view our approach does *not* imply that the Dirac vector and scalar densities of the target have been taken to be identical. With ψ_- set to zero, Eq. (A17) yields

$$\rho_V(q) \approx \int d^3p\, u^\dagger(\mathbf{p}-\tfrac{1}{2}\mathbf{q},+) u(\mathbf{p}+\tfrac{1}{2}\mathbf{q},+) \times \psi_+^\dagger(\mathbf{p}-\tfrac{1}{2}\mathbf{q}) \psi_+(\mathbf{p}+\tfrac{1}{2}\mathbf{q}) , \tag{A24}$$

for the vector density in momentum space, and

$$\rho_S(q) \approx \int d^3p\, \bar{u}(\mathbf{p}-\tfrac{1}{2}\mathbf{q},+) u(\mathbf{p}+\tfrac{1}{2}\mathbf{q},+) \times \psi_+^\dagger(\mathbf{p}-\tfrac{1}{2}\mathbf{q}) \psi_+(\mathbf{p}+\tfrac{1}{2}\mathbf{q}) , \tag{A25}$$

for the scalar density in momentum-space. These expressions are not equal. This is because neglect of negative energy plane-wave components does not imply neglect of lower components. We also note that because our optimum factorization procedure involves removal of the complete t-matrix element from the folding integral of Eq. (A19), the Dirac plane-wave spinors for the expansion of the initial and final state of the bound nucleon have also been removed from the folding integral. Thus quantities such as those in Eqs. (A24) and (A25) do not appear explicitly in our present calculations. Only *one* piece of shape information, namely that in Eq. (A21) enters. If one had firmer knowledge of the Dirac NN operator t_D, then it would be possible to implement optimum factorization by removing just t_D from the integral, leaving expressions such as those in Eqs. (A24) and (A25) which would be more closely comparable to the standard Dirac vector and scalar densities. Since ψ_- is very small, a large part of the difference between Dirac vector and scalar densities derives from the different Dirac plane-wave spinor matrix elements in Eqs. (A24) and (A25). Effectively, these matrix elements (albeit, evaluated at $\mathbf{p}=0$) have been included in the complete t-matrix elements that we deal with. Thus, from the point of view of previous approaches, a large part of difference between vector and scalar target densities has been included implicitly in the calculations reported here. The studies of the sensitivity of results to small changes in the relative strength of vector and scalar optical potentials presented in the text intentionally do not attribute this sensitivity to either the t matrix or the density in isolation, since only the combination can be identified at the present level of treatment.

[1] A. Picklesimer, P. C. Tandy, R. M. Thaler, and D. H. Wolfe, Phys. Rev. C **29**, 1582 (1984); **30**, 1861 (1984).

[2] J. R. Shepard, J. A. McNeil, and S. J. Wallace, Phys. Rev. Lett. **50**, 1443 (1983); B. C. Clark, S. Hama, R. L. Mercer, L. Ray and B. D. Serot, *ibid.* **50**, 1644 (1983).

[3] L. S. Celenza and C. M. Shakin, Phys. Rev. C **29**, 1784 (1984).

[4] Some initial results from the relativistic calculations described in this paper have been published in M. V. Hynes, A. Picklesimer, P. C. Tandy, and R. M. Thaler, Phys. Rev. Lett. **52**, 978 (1984). Since the publication of that work, we have discovered a numerical instability in some of the high momentum transfer (high q) results reported therein. None of the conclusions of that work are changed. Only the detailed features of the high q predictions at 500 MeV, shown in the figures, are changed. This problem is corrected in the present work and extensive numerical tests indicate that our high q results are now completely stable.

[5] K. M. Watson, Phys. Rev. **89**, 575 (1953); N. C. Francis and K. M. Watson, *ibid.* **92**, 291 (1953).

[6] Strongly excited collective states go as n/A, where n is the effective number of excited nucleons, rather than $1/A$, and are obvious exceptions to these considerations if n/A is not small. In such a situation a coupled channel approach is required.

[7] G. E. Brown and D. G. Ravenhall, Proc. R. Soc., London, Sect. A **208**, 552 (1951); J. Sucher, Rep. Prog. Phys. **41**, 1781 (1978); Phys. Rev. A **22**, 348 (1980); J. Sucher, in *Proceedings of the NATO Advanced Study Institute on Relativistic Effects in Atoms, Molecules, and Solids, Vancouver, 1981,* edited by G. Malli (Plenum, New York, 1983).

[8] J. A. McNeil, L. Ray, and S. J. Wallace, Phys. Rev. C **27**, 2123 (1983).

[9] J. D. Bjorken and S. D. Drell, *Relativistic Quantum Mechanics* (McGraw-Hill, New York, 1964).

[10] A. K. Kerman, H. McManus, and R. M. Thaler, Ann. Phys. (N.Y.) **8**, 551 (1959); A. Picklesimer and R. M. Thaler, Phys. Rev. C **23**, 42 (1981).

[11] For relativistic treatments of nuclear matter that have this starting point see, e.g., M. R. Anastasio, L. S. Celenza, W. S. Pong, and C. M. Shakin, Phys. Rep. **100**, 327 (1983).

[12] J. A. Tjon and S. J. Wallace (private communication).

[13] The integral equation formulation suggests generalizations to include physical effects that lie outside the scope of a one-body Dirac equation. For example, the influence of target recoil may be included by replacing Eq. (24) with $\Gamma_\pm(k'') = [E - E_A(k'') \mp (E_{k''})]^{-1}$, where $E_A(k'')$ is the total energy of the nucleus when the projectile has momentum k'' in the frame of zero total momentum. We have employed these propagators in the numerical calculations. These effects of target recoil are not significant. With relativistic N-nucleus interactions defined in terms of target matrix elements of NN operators, the effects of a nonzero spin target would apparently enter with the use of the appropriate target spinor in much the same way as in the nonrelativistic case. The quantities U and T in the integral Eqs. (22) and (23) would then have the appropriate multiplet structure for total spin. The original Dirac equation which describes a spin $\frac{1}{2}$ doublet, does not suggest an unambiguous generalization.

[14] The general form for the Dirac optical potential operator consistent with invariance principles has been given in L. S. Celenza and C. M. Shakin, Phys. Rev. C **28**, 1256 (1983).

[15] L. G. Arnold and B. C. Clark, Phys. Lett. **84B**, 46 (1979); B. C. Clark, in *Interaction Between Medium Energy Nucleons*

and Nuclei—1982, Proceedings of the Workshop on the Interaction Between Medium Energy Nucleons in Nuclei, Indiana University, 1982, AIP Conf. Proc. No. 97, edited by H. O. Meyer (AIP New York, 1983).

[16]J. D. Walecka, Ann. Phys. (N.Y.) **83**, 491 (1974); C. J. Horowitz and B. D. Serot, Nucl. Phys. **A368**, 503 (1981).

[17]This effective nonrelativistic form of the Dirac equation has been employed recently to discuss the extrapolation from relativistic bound state calculations to Schrödinger optical potentials in M. R. Anastasio, L. S. Celenza, and C. M. Shakin, Phys. Rev. C **23**, 2606 (1981).

[18]C. W. DeJager, M. DeVries, and C. DeVries, At. Data Nucl. Data Tables **14**, 479 (1974).

[19]J. Kelley *et al.*, Phys. Rev. Lett. **45**, 2012 (1980).

[20]B. Aas (private communication).

[21]B. A. Brown, Michigan State shell model code (private communication).

[22]B. B. P. Sinha *et al.*, Phys. Rev. C **7**, 1930 (1973); I. Sick and J. S. McCarthy, Nucl. Phys. **A150**, 631 (1970).

[23]D. J. Ernst and G. A. Miller, Phys. Rev. C **21**, 1472 (1980).

[24]G. W. Hoffman *et al.*, Phys. Rev. Lett. **47**, 1436 (1981); A. Rahbar *et al.*, Phys. Rev. Lett. **47**, 1811 (1981).

[25]L. G. Arnold, B. C. Clark, R. L. Mercer, and P. Schwandt, Phys. Rev. C **23**, 1949 (1981).

[26]M. V. Hynes and B. Aas, Los Alamos National Laboratory Report No. LA-9709-PR, 1982 (unpublished).